細胞表面の抗体染色による細胞内シグナルへの影響など、注意しなければならない点もあるが、今後ヒトB細胞亜集団の解析を行なう有用な手段である。

E. 結　論

1. SCID マウスへの移植実験によりマウス胎児肝共通リンパ球前駆細胞が B-1 細胞に特化した分化能を持つことが初めて明らかとなった。

2. マウス胎児肝 Lin-細胞から CD19+ B220- B-1 前駆細胞を分化させる培養系を樹立した。その際、CD19+ B220-細胞に先立ちCD19+ B220+細胞が出現することが明らかとなった。

3. マウス腹腔内のB-1細胞とB-2細胞の抗原受容体架橋時のカルシウムイオン濃度の変化に違いがあることが明らかとなった。

F. 健康危機情報

なし

G. 研究発表

1. 論文発表

該当なし

2. 学会発表

KOURO Taku, IKUTANI Masashi, TERATANI Akie, NAGAI Yoshinori, TAKATSU Kiyoshi. B-1 cell-restricted differentiation of IL-7R+ lymphoid progenitors from fetal liver. 第３８回日本免疫学会学術集会，２００８年１２月１日ー３日，京都

(発表誌名巻号・頁・発行年等も記入)

H. 知的財産権の出願・登録状況 (予定を含む)

1. 特許取得

該当なし

2. 実用新案登録

該当なし

3. その他

なし

Ⅳ. 研究成果の刊行に関する一覧表

研究成果の刊行に関する一覧表 平成20年度(2008)

〈雑誌〉

主任研究者:清野 宏

発表者氏名	論文タイトル名	発表雑誌名	巻	頁	出版年
Terahara, K., Yoshida, M., Igarashi, O., Nochi, T., Pontes, G. S., Hase, K., Ohno, H., Kurokawa, S., Mejima, M., Takayama, N., Yuki, Y., Lowe, A. W., and Kiyono, H.	Comprehensive gene expression profiling of Peyer's patch M cells, villous M-like cells, and intestinal epithelial cells.	J. Immunol.	180	7840-7846	2008
Momoi F, Hashizume T, Kurita-Ochiai T, Yuki Y, Kiyono H and Yamamoto M.	Nasal vaccination with outer membrane protein of *Porphyromonas gingivalis* and nontoxic chimeric enterotoxin adjuvant induces long-term protective immunity with reduced IgE antibodies.	Infect. Immun.	76	2777-2784	2008
Kunisawa J, Gohda M, Kurashima Y, Ishikawa I, Higuchi M and Kiyono H.	Sphingosine 1-phosphate-dependent trafficking of peritoneal B cells requires functional NFk B-inducing kinase in stromal cells.	Blood	111	4646-4652	2008
Gohda M, Kunisawa J, Miura F, Kagiyama Y, Kurashima Y, Higuchi M, Ishikawa I, Ogahara I and Kiyono H.	Sphingosine 1-phosphate regulates the egress of IgA plasmablasts from Peyer's patches for intestinal IgA responses.	J. Immunol.	180	5335-5343	2008
Chang SY,Cha HR,Uematsu S,Akira S, Igarashi O, Kiyono H and Kweon MN.	Colonic patches direct the cross-talk between systemic compartments and large intestine independently of innate immunity.	J. Immunol.	180	1609-1618	2008

Caipang CM, Verjan N, Ooi EL, Kondo H, Hirono I, Aoki T, Kiyono H and Yuki Y.	Enhanced survival of shrimp, *Penaeus (Marsupenaeus) japonicus* from white spot syndrome disease after oral administration of recombinant VP28 expressed in *Brevibacillus brevis*.	Fish Shellfish Immunol.	25	315-320	2008
Ooi EL, Verjan N, Haraguchi I, Oshima T, Kondo H, Hirono I, Aoki T, Kiyono H and Yuki Y.	Innate immunomodulation with recombinant interferon-alpha enhances resistance of rainbow trout (*Oncorhynchus mykiss*) to infectious hematopoietic necrosis virus.	Dev. Comp. Immunol.	32	1211-1220	2008
Hashizume T, Togawa A, Nochi T, Igarashi O, Kweon MN, Kiyono H and Yamamoto M.	Peyer's patches are required for intestinal IgA responses to *Salmonella*.	Infect. Immun.	76	927-934	2008
Uematsu S, Fujimoto K, Jang MH, Yang BG, Jung YJ, Nishiyama M, Sato S, Tsujimura T, Yamamoto M, Yokota Y, Kiyono H, Miyasaka M, Ishii KJ and Akira S.	Regulation of humoral and cellular gut immunity by lamina propria dendritic cells expressing Toll-like receptor 5.	Nat. Immunol.	9	769-776	2008
Verjan N, Ooi EL, Nochi T, Kondo H, Hirono I, Aoki T, Kiyono H and Yuki Y.	A soluble nonglycosylated recombinant infectious hematopoietic necrosis virus (IHNV) G-protein induces IFNs in rainbow trout (*Oncorhynchus mykiss*).	Fish Shellfish Immunol.	25	170-180	2008
Kobayashi T, Takahashi K, Nagai Y, Shibata T, Otani M, Izui S, Akira S, Gotoh Y, Kiyono H and Miyake K.	Tonic B cell activation by radioprotective105/MD-1 promotes disease progression in MRL/lpr mice.	Int. Immunol.	20	881-891	2008
Chang SY, Cha HR, Igarashi O, Rennert PD, Kissenpfennig A, Malissen B, Nanno M, Kiyono H and Kweon MN.	Cutting edge: langerin+ dendritic cells in the mesenteric lymph node set the stage for skin and gut immune system cross-talk.	J. Immunol.	180	4361-4365	2008

Ooi EL, Verjan N, Hirono I, Nochi T, Kondo H, Aoki T, Kiyono H and Yuki Y.	Biological characterisation of a recombinant Atlantic salmon type I interferon synthesized in *Escherichia coli*.	Fish Shellfish Immunol.	24	506-513	2008
Fehervari Z and Kiyono H.	The mucosa: at the frontlines of immunity.	Trends Immunol.	in press	in press	2008
Kunisawa J, Nochi T and Kiyono H.	Immunological commonalities and distinctions between airway and digestive immunity.	Trends Immunol.	in press	in press	2008

分担研究者：寺尾　恵治

発表者氏名	論文タイトル名	発表雑誌名	巻	頁	出版年
Terao K.	Dynamic changes in early development of immune system in macaque monkeys –The significance from standpoint of the preclinical toxicity test using nonhuman primates-.	J. Toxicol. Science	in press	in press	2009

〈書籍〉

主任研究者：清野宏

著者氏名	論文タイトル名	書籍全体の編集者名/書籍名	出版社名・出版地	頁	出版年
Kiyono, H., Kunisawa, J., McGhee, J. R., and Mestecky,J.	The mucosal immune system.	In Fundamental Immunology (Edited by William E. Paul).	Lippincott-Raven, Philadelphia	983-1030	2008

Ⅴ．研究成果の刊行物・別冊
（主なもの）

Comprehensive Gene Expression Profiling of Peyer's Patch M Cells, Villous M-Like Cells, and Intestinal Epithelial Cells[1]

Kazutaka Terahara,[2*‡] Masato Yoshida,[2*†] Osamu Igarashi,[*‡] Tomonori Nochi,[*‡] Gemilson Soares Pontes,[*] Koji Hase,[§] Hiroshi Ohno,[§] Shiho Kurokawa,[*] Mio Mejima,[*] Naoko Takayama,[*†] Yoshikazu Yuki,[*‡] Anson W. Lowe,[¶] and Hiroshi Kiyono[3*†‡]

Separate populations of M cells have been detected in the follicle-associated epithelium of Peyer's patches (PPs) and the villous epithelium of the small intestine, but the traits shared by or distinguishing the two populations have not been characterized. Our separate study has demonstrated that a potent mucosal modulator cholera toxin (CT) can induce lectin *Ulex europaeus* agglutinin-1 and our newly developed M cell-specific mAb NKM 16-2-4-positive M-like cells in the duodenal villous epithelium. In this study, we determined the gene expression of PP M cells, CT-induced villous M-like cells, and intestinal epithelial cells isolated by a novel approach using FACS. Additional mRNA and protein analyses confirmed the specific expression of glycoprotein 2 and myristoylated alanine-rich C kinase substrate (MARCKS)-like protein by PP M cells but not CT-induced villous M-like cells. Comprehensive gene profiling also suggested that CT-induced villous M-like cells share traits of both PP M cells and intestinal epithelial cells, a finding that is supported by their unique expression of specific chemokines. The genome-wide assessment of gene expression facilitates discovery of M cell-specific molecules and enhances the molecular understanding of M cell immunobiology. *The Journal of Immunology*, 2008, 180: 7840–7846.

As a unique epithelial cell type specializing in Ag sampling, microfold or membranous cells (M cells) are present in the follicle-associated epithelium (FAE)[4] of both GALT and nasopharynx-associated lymphoid tissue, which act as a major inductive site for Ag-specific mucosal immune responses (1, 2). Recently, we also identified M cells in the small intestinal villous epithelium, at effector sites far from the FAE, suggesting that Ag sampling via villous M cells may be responsible for induction of systemic Ag-specific immune responses, such as IgG production via the oral route (3). Still missing, however, were a characterization of the shared and distinctive traits of Peyer's patches (PPs) and villous M cells and a better understanding of the immunological nature of each.

Recent comprehensive gene expression analyses using microdissected FAE or whole cells dissociated from the FAE identified genes specifically expressed by PP M cells (4–6). Similar data, however, have not been available for villous M cells, in part because sufficient numbers of M cells are difficult to isolate from the surrounding intestinal epithelial cells (IECs). In mice, lectin *Ulex europaeus* agglutinin-1 (UEA-1) possessing affinity for α (1, 2) fucose has been routinely used for the detection of such M cells (3, 7). UEA-1, however, does not alone suffice to identify M cells because it also reacts to goblet cells (3). Our laboratory has recently succeeded in distinguishing M cells from goblet cells by developing a mAb (NKM 16-2-4 mAb) that specifically reacts to murine PP and villous M cells but not goblet cells and IECs (8). Furthermore, our recent separate studies have demonstrated that oral administration of cholera toxin (CT) as mucosal adjuvant resulted in the induction of NKM 16-2-4 mAb$^+$ and UEA-1$^+$ M-like cells, which have pocket structure and Ag uptake ability, in the duodenal villous epithelium (Terahara et al., submitted for publication). These recent advances in our understanding of M cells allowed us to define gene expression profiles capable of distinguishing PP M cells, CT-induced villous M-like cells, and IECs.

Materials and Methods

Animals

BALB/c mice were purchased from Japan SLC. These mice were maintained under specific pathogen-free conditions in horizontal flow cabinets in our experimental animal facility at the University of Tokyo. Following a previously established protocol (9, 10), CT (List Biologic Laboratories) was dissolved in PBS (20 μg/mouse) and then orally administered to BALB/c mice. Two days after CT administration, mice were used for experiments. All animal experiments were approved by the Animal Care and Use Committee of University of Tokyo.

Lectins and Abs for the detection of M cells

The following fluorescence-conjugated lectins and Abs were used for the identification of PP and villous M cells by FACS and histochemistry: PE-conjugated UEA-1 (Biogenesis), rhodamine-conjugated UEA-1 (Vector

*Division of Mucosal Immunology, Department of Microbiology and Immunology, The Institute of Medical Science and [†]Department of Medical Genome Science, Graduate School of Frontier Science, The University of Tokyo, Tokyo, [‡]Core Research for Evolutional Science and Technology, Japan Science and Technology Corporation, Saitama, and [§]Laboratory of Epithelial Immunobiology, Research Center for Allergy and Immunology, Institute of Physical and Chemical Research, Yokohama, Japan; and [¶]Department of Medicine, Stanford University, Stanford, CA 94305

Received for publication February 12, 2007. Accepted for publication April 3, 2008.

The costs of publication of this article were defrayed in part by the payment of page charges. This article must therefore be hereby marked *advertisement* in accordance with 18 U.S.C. Section 1734 solely to indicate this fact.

[1] This work was supported in part by grants from Core Research for Evolutional Science and Technology of the Japan Science and Technology Corporation, the Ministry of Education, Science, Sports, and Culture, and the Ministry of Health and Welfare in Japan.

[2] K.T. and M.Y. contributed equally to this work and share first authorship.

[3] Address correspondence and reprint requests to Dr. Hiroshi Kiyono, Division of Mucosal Immunology, Department of Microbiology and Immunology, The Institute of Medical Science, The University of Tokyo, 4-6-1 Shirokanedai, Minato-ku, Tokyo 108-8639, Japan. E-mail address: kiyono@ims.u-tokyo.ac.jp

[4] Abbreviations used in this paper: FAE, follicle-associated epithelium; 7-AAD, 7-amino actinomycin; CKLF, chemokine-like factor; CT, cholera toxin; DAPI, 4′-6-diamidino-2-phenylindole; IEC, intestinal epithelial cell; IEL, intraepithelial lymphocyte; ISH, in situ hybridization; MLP, myristoylated alanine-rich C kinase substrate (MARCKS)-like protein; PP, Peyer's patch; UEA-1, *Ulex europaeus* agglutinin-1; WGA, wheat germ agglutinin.

Laboratories), biotin-conjugated UEA-1 (Vector Laboratories), FITC-conjugated wheat germ agglutinin (WGA) (Vector Laboratories), FITC-conjugated or biotin-conjugated M cell-specific NKM 16-2-4 mAb (8), and allophycocyanin-Cy7-conjugated anti-mouse CD45 mAb (30-F11; BD Biosciences).

Isolation of PP M cells, CT-induced villous M-like cells, and IECs

PPs from the naive duodenum and PP-free segments from the duodenum of naive or CT-administered mice were washed with cold PBS. Cells were dissociated from the small intestinal epithelium using a previously described mechanical procedure with some modifications (11). In brief, the tissues were incubated in PBS containing 0.5 mM EDTA with a stirrer for 10 min at 37°C. More than 90% of the dissociated cells survived as confirmed by a trypan blue exclusion test. The cells were stained with 1 μg/ml FITC-conjugated NKM 16-2-4 mAb, 5 μg/ml PE-conjugated UEA-1, and 1 μg/ml allophycocyanin-Cy7-conjugated anti-mouse CD45 mAb for 40 min before being reacted with 7-amino actinomycin (7-AAD; BD Biosciences) diluted 1/5 in DMEM containing 10% FCS for 10 min on ice. After washing with DMEM containing 10% FCS, the stained cells were analyzed using a flow cytometer FACSAria (BD Biosciences), and suitable cell populations gated on $CD45^-$ and $7\text{-}AAD^-$ cells were sorted.

DNA microarray analysis

Total RNA was extracted from the freshly isolated PP M cells, CT-induced villous M-like cells, and IECs of BALB/c mice using a High Pure RNA Tissue kit (Roche). Biotinylated cRNA was prepared using a two-cycle target-labeling assay in accordance with the protocol of the manufacturer (Affymetrix). The cRNA was hybridized with DNA probes on a GeneChip Mouse Genome 430 2.0 array (Affymetrix), washed, and fluorescence-labeled in accordance with the standard amplification protocol for eukaryotic targets developed by Affymetrix. The arrays were scanned with a GeneChip Scanner 3000 7G (Affymetrix). The fluorescence intensity of each probe was taken to represent the raw expression level and was quantified using GeneChip Operating software (Affymetrix). Data obtained from three independent experiments for PP M cells, CT-induced villous M-like cells, and IECs were normalized and statistically analyzed by Welch's ANOVA using GeneSpring 7.3.1 software (Silicon Genetics). In addition, both qualitative indices ("Present Call," "Marginal Call," and "Absent Call") based on *p*-value and a quantitative index (raw value) were also determined using GeneSpring 7.3.1 software. All microarray data described in this study have been deposited in the National Center for Biotechnology Information Gene Expression Omnibus database (www.ncbi.nlm.nih.gov/geo/) with the accession no. GSE7838.

In situ hybridization (ISH)

DNA fragments encoding GP2 (GenBank: NM_025989) and myristoylated alanine-rich C kinase substrate (MARCKS)-like protein (MLP; GenBank: NM_010807) were amplified by PCR from PP FAE-derived cDNA. The following sets of primers were used: *GP2*, sense, 5′-GGGTGATGGAGG AGTGAAGA-3′, anti-sense, 5′-CTCCAGGATGTTCCCACAGT-3′; and *MLP*, sense, 5′-*AATTAACCCTCACTAAAGGG*GAAGGCCAACGGACAG GAGA-3′, anti-sense, 5′-*TAATACGACTCACTATAGGGC*TTCTTGGGG GTCTCCTTGG-3′ (T3 and T7 promoter sequences are shown by italics). The PCR products for GP2 were subcloned into a pCR4-TOPO vector (Invitrogen). After sequencing, digoxigenin-labeled sense and anti-sense RNA probes were transcribed in vitro from the subcloned plasmids or from T3 and T7 promoter-conjugated PCR products with DIG RNA labeling mix (Roche). Paraffin-embedded sections of small intestinal tissues (6 μm) from naive BALB/c mice were obtained from Genostaff. ISH was performed as previously described (12). The bound probes were detected with BM purple AP substrate (Roche), before being counterstained with Kernechtrot stain solution (Muto Pure Chemicals) or reacted with 0.25 μg/ml biotin-conjugated UEA-1 at 4°C overnight after treatment with 3% H_2O_2. The sections labeled with biotin-conjugated UEA-1 were further reacted with HRP-conjugated streptavidin, followed by staining with 3,3′ diaminobenzidine (Vector Laboratories).

Generation of GP2- and MLP-specific Abs

For the generation of GP2- and MLP-specific Abs, the open reading frames of *GP2* and *MLP* genes were amplified by PCR from PP FAE-derived cDNA. The following sets of primers were used: *GP2*, sense, 5′-GACA T*GCTAGC*ATGAAAAGGATGGTGGGTTGTGAC-3′, anti-sense, 5′-GT ATC*GAATTC*TCAGAACAGTAGAGCCAGGAAGAC-3′; and *MLP*, sense, 5′-TGACT*GAATTC*ATGGGCAGCCAGAGCTCTAAGGCT-3′, anti-sense, 5′-TACAT*GTCGAC*CTACTCATTCTGCTCAGCACTGGC-3′,

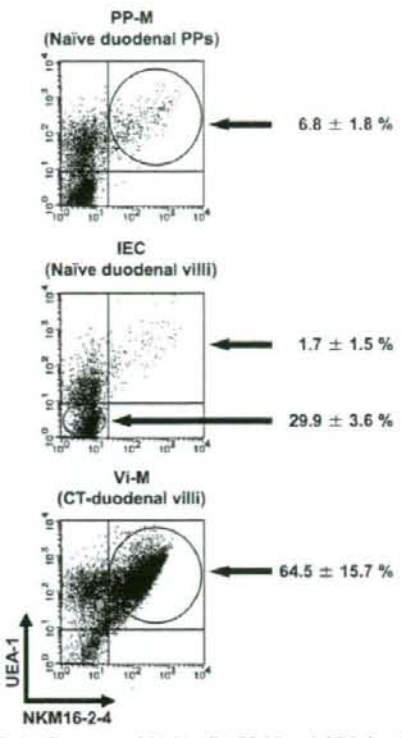

FIGURE 1. Frequency of PP M cells (PP-M) and CT-induced villous M-like cells (Vi-M) in the duodenal epithelium. Dot plots are shown by NKM 16-2-4-FITC and UEA-1-PE staining gated on $CD45^-$ and $7\text{-}AAD^-$ duodenal epithelial cell populations from naive BALB/c mice or from those that had been orally treated with CT. PP-M (NKM 16-2-4$^+$ and UEA-1$^+$), Vi-M (NKM 16-2-4$^+$ and UEA-1$^+$), and IEC (NKM 16-2-4$^-$ and UEA-1$^-$) were isolated by FACS. Numbers are the mean percentage ± SD in $CD45^-$ and $7\text{-}AAD^-$ epithelial cell populations from three independent experiments.

[*Nhe*I and *Eco*RI (*GP2*), and *Eco*RI and *Sal*I (*MLP*) restriction enzyme sites are shown by italics]. For generation of GP2-specific mAbs, amplified *GP2* gene was subcloned into pIRES2-EGFP vector (BD Biosciences) and the plasmid (pIRES2-GP2-EGFP) was then introduced in rat IEC line IEC-6 (ATCC, CRL-1592). After 2 days of transformation, EGFP-positive cells were purified by FACSAria and injected into the footpads of SD rats (1×10^6 cells/rat) five times at 2-wk intervals with TiterMax Gold (TiterMax) as an adjuvant. Four days after the final immunization, lymphocytes isolated from inguinal lymph node of the immunized rats were fused with P3×63-AG8.653 myeloma cells (ATCC, CRL-1580) in the presence of 50% (w/v) polyethylene glycol 1500 (Roche). Established hybridomas were injected into Crlj; CD1-*Foxn1*^{nu} mice and mAbs were purified from ascites by using Protein G-Sepharose (GE Healthcare). For generation of MLP-specific polyclonal Abs, the amplified *MLP* gene was subcloned into pGEX-4T-1 (GE Healthcare) and the plasmid (pMLP-GEX-4T-1) was then introduced in *Escherichia coli* DH5α. After induction of MLP expression with 0.1 mM isopropyl β-D-thiogalactoside, the GST-fused MLP was purified on a Glutathione-Sepharose 4B (GE Healthcare) and subsequently removed the GST-tag with thrombin (GE Healthcare). The purified rMLP was then immunized into New Zealand white rabbits and anti-MLP pAbs were purified from the antiserum by using rMLP-conjugated TOYOPEARL AF-Tresyl-650M (Tosoh).

Histochemical analysis

The histochemical analyses were performed with whole-mount tissues and frozen-section specimens prepared from mucus-free tissues fixed with 4% paraformaldehyde in PBS as previously described (3). For GP2 staining,

A

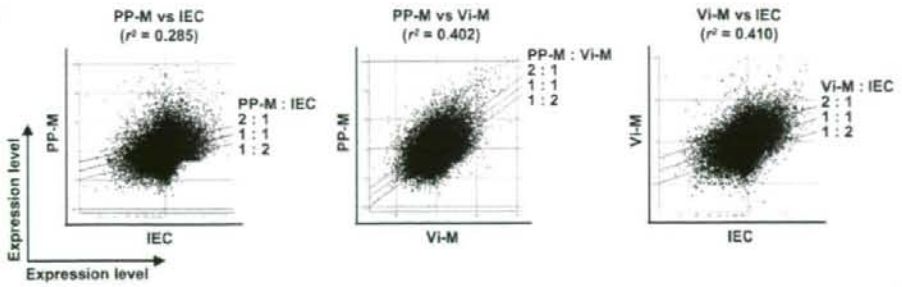

B

Group	Description	Criterion
A	PP-M-significant	1. "Present" or "Marginal Call" together with ≥ 100 raw value is shown in a cell fraction but not in the other two cell fractions. 2. A normalized expression signal in a cell fraction is two-fold or higher than that seen in the other two cell fractions.
B	Vi-M-significant	
C	IEC-significant	
D	Sharing between PP-M and Vi-M	1. "Present" or "Marginal Call" together with ≥ 100 raw value is shown in two cell fractions but not in another cell fraction. 2. Each normalized expression signal in two cell fractions is two-fold or higher than that in another cell fraction.
E	Sharing between PP-M and IEC	
F	Sharing between Vi-M and IEC	
G	Sharing in all cell fractions	1. "Present" or "Marginal Call" together with ≥ 100 raw value is shown in all cell fractions.

C

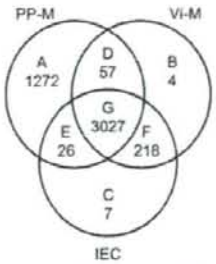

FIGURE 2. Gene expression profiles for PP M cells (PP-M), CT-induced villous M-like cells (Vi-M), and IECs. *A*, Scatter plots of the normalized expression level on each DNA microarray probe for PP-M and IEC, PP-M and Vi-M, and Vi-M and IEC with correlation coefficients (r^2). *B*, Grouping of probes based on their significance for PP-M, Vi-M, and IEC using the criteria outlined in the qualitative ("Present Call" or "Marginal Call") and quantitative (raw value) indices as assessed by GeneSpring 7.3.1 software. *C*, Venn diagram showing the categorization of significant probes into seven groups (Group A–G).

the specimens were incubated with 1 μg/ml rat anti-GP2 mAb (10F5-9-2) or the isotype control Ab (rat IgG2a; BD Biosciences) at 4°C overnight. For MLP staining, tissue sections were incubated with 10 μg/ml anti-MLP pAb or normal rabbit IgG at 4°C overnight. The specimens were then treated with 3 μg/ml Cy5-conjugated donkey anti-rat IgG or 3 μg/ml Cy5-conjugated donkey anti-rabbit IgG (Jackson ImmunoResearch Laboratories) together with 10 μg/ml tetramethylrhodamine isothiocyanate-conjugated UEA-1 (Vector Laboratories) and/or 5 μg/ml FITC-conjugated WGA (Vector Laboratories) for 1 h at room temperature. Finally, the section specimens were reacted with 400 ng/ml 4′-6-diamidino-2-phenylindole (DAPI; Sigma-Aldrich) and the signal was observed under a confocal laser-scanning microscope (TCS SP2; Leica). For counterstaining with our recently established M cell-specific mAb (NKM 16-2-4; rat IgG2c), the same section specimens were incubated with 5 μg/ml biotin-conjugated NKM 16-2-4 at 4°C overnight followed by 1.25 μg/ml HRP-conjugated streptavidin (Pierce) for 1 h at room temperature. The signal was then developed with 3,3′ diaminobenzidine and the nucleus was finally stained with hematoxylin.

Results

Isolation of PP M cells, CT-induced villous M-like cells, and IECs by FACS

FACS analysis demonstrated that the large forward-scatter $CD45^-$ cell population could be divided into three subpopulations by NKM 16-2-4 mAb and UEA-1 staining (Fig. 1). Because of the known specificities of NKM 16-2-4 mAb and UEA-1, cells positive for NKM 16-2-4 and UEA-1 were identified as M cells (or M-like cells) in this study. In the $CD45^-$ epithelial cell population isolated from the duodenum of naive BALB/c mice, the frequency of PP M cells averaged 7%. Perhaps due to the nature of the isolation technique used, the harvest of PP M cells far outstripped that of villous M cells, the frequency of the latter being so low (1.7 ± 1.5%) as to render harvest extremely difficult. We recently found that the number of villous M-like cells could be increased by oral administration of CT (64.5 ± 15.7% and Terahara et al., submitted for publication), and so decided to use the villous M-like cells induced by CT treatment for this DNA microarray analysis. A FACS with a purity of 90–99% was used to isolate PP M cells (NKM 16-2-4^+/UEA-1^+), CT-induced villous M-like cells (NKM 16-2-4^+/UEA-1^+), and IECs (NKM 16-2-4^-/UEA-1^-).

Assessment of gene expression profiling of PP M cells, CT-induced villous M-like cells, and IECs

DNA microarrays containing 45,101 probes were used to determine the comprehensive gene expression of PP M cells, CT-induced villous M-like cells, and IECs. Comparison of these

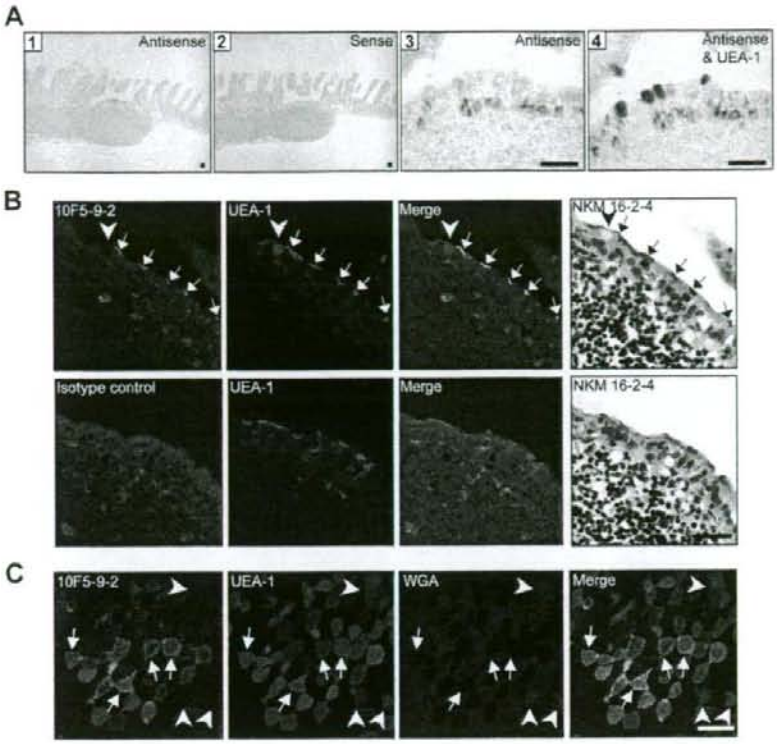

FIGURE 3. GP2 was specifically expressed by PP M cells in the small intestine. *A*, ISH for GP2 mRNA with positive signals (blue) of hybridized anti-sense or sense cRNA probes on duodenal PPs and adjacent villi of naive BALB/c mice. Tissues were also counterstained with Kernechtrot (pink, *1* and *2*) or labeled with UEA-1-HRP before being stained with 3,3' diaminobenzidine (brown, *4*). *3* and *4*, High magnification of a PP FAE before (*3*) and after (*4*) labeling with UEA-1. Scale bar = 200 μm (*1* and *2*) and 40 μm (*3* and *4*). *B*, Confocal images of frozen sections of PPs stained with anti-GP2-specific mAb (10F5-9-2) or isotype control (rat IgG2a). The specific expression of GP2 in M cells was confirmed by counterstaining with our recently established M cell-specific mAb (NKM 16-2-4). Arrows and arrowheads show M cells and goblet cells, respectively. Scale bar = 30 μm. *C*, Confocal images of whole-mount duodenal PP domes stained with anti-GP2-specific mAb (10F5-9-2), UEA-1, and WGA. Scale bar = 30 μm.

profiles revealed correlation coefficients of 0.285 for PP M cells and IECs, of 0.402 for PP M cells and CT-induced villous M-like cells, and of 0.410 for CT-induced villous M-like cells and IECs (Fig. 2*A*). Based on the constructed gene profiling, we categorized probes showing significant expression into seven groups (Groups A-G) using our own criteria (Fig. 2*B*). The 1272, 4, and 7 probes were regarded as significant for PP M cells (Group A), CT-induced villous M-like cells (Group B), and IECs (Group C), respectively (Fig. 2*C*). The relative expression levels and gene names of the significant probes are provided in Supplementary Table I.[5] Our gene-profiling database allowed us to confirm previous findings that Group A includes the transcripts of peptidoglycan recognition protein-S, secretory granule neuroendocrine protein 1, and annexin V that are specifically expressed by PP M cells (4–6).

Specific expression of GP2 by PP M cells

In an effort to identify molecules that could be expressed on the apical surface of PP M cells, we looked for genes showing a higher expression level in Group A. During the ISH analysis, we found that GP2 mRNA was specifically expressed in the FAE of PPs throughout the small intestine (Fig. 3*A*, *1*) and that its expression was distinctively colocalized with UEA-1$^+$ M cells (Fig. 3*A*, *3* and *4*). A negative control using sense cRNA probes did not show any positive signals (Fig. 3*A*, *2*). Immunohistochemical analysis with newly established anti-GP2-specific mAb (10F5-9-2) revealed that the GP2 protein was highly expressed in UEA-1$^+$ PP M cells (Fig. 3*B*). A negative control using isotype rat IgG2a did not show any positive signals in the dome epithelium of PPs (Fig. 3*B*). The expression of GP2 in M cells was further confirmed by counterstaining with our recently established M cell-specific mAb NKM 16-2-4 (Fig. 3*B*). Supporting the histochemical analyses, whole-mount staining analysis also demonstrated GP2 was expressed on the apical surface of UEA-1$^+$ PP M cells, which were not recognized by enterocyte-reactive lectin WGA (Fig. 3*C*). Supporting the gene profiling data (Supplementary Table I), GP2 protein was not detected in CT-induced villous M-like cells (data not shown).

Unique expression of MLP by PP M cells in the small intestine

Candidates for FAE-specific genes including *MLP* (also known as *MacMARCKS* or *MRP*) have been previously proposed (5, 6). Most of these genes together with *MLP* could be identified as PP M cell-significant genes by the DNA microarray analysis (Supplementary Table I). The subsequent ISH analysis demonstrated a unique expression pattern of MLP mRNA in the small intestine, i.e., MLP mRNA was detected in the FAE and B cell zones of PPs throughout the small intestine (Fig. 4*A*, 1). A negative control using sense cRNA probes did not show any positive signals (Fig. 4*A*, 2). In the FAE, the expression of MLP mRNA was exclusively colocalized with UEA-1$^+$ M cells (Fig. 4*A*, 3 and 4). Immunohistochemical analysis further elucidated the complicated expression pattern of MLP, revealing that the MLP protein was also found in B cell zones and the cytoplasm of M cells in PPs throughout the small intestine (Fig. 4*B*), but not in CT-induced villous M-like cells (data not shown). A negative control using normal rabbit IgG did not show any positive signals (Fig. 4*B*).

[5] The online version of this article contains supplemental material.

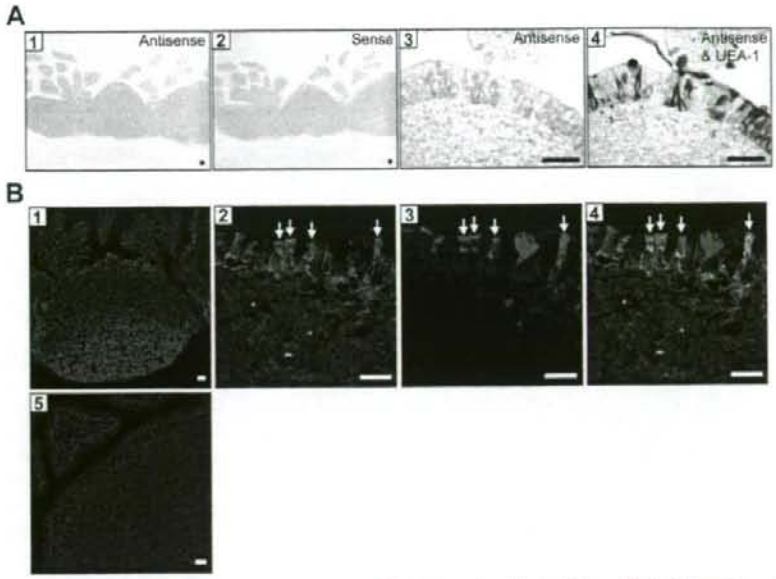

FIGURE 4. MLP was expressed by M cells and by the B cell zones of PPs but not by villi. *A*, ISH for MLP mRNA with positive signals (blue) of hybridized anti-sense or sense cRNA probes on duodenal PPs and adjacent villi of naive BALB/c mice. Tissues were also counterstained with Kernechtrot (pink, *1* and *2*) or labeled with UEA-1-HRP before being stained with 3,3' diaminobenzidine (brown, *4*). *3* and *4*, High magnification of a PP FAE before (*3*) and after (*4*) labeling with UEA-1. Scale bar = 200 μm (*1* and *2*) and 40 μm (*3* and *4*). *B*, Confocal images of frozen sections of duodenal PPs stained with anti-MLP-specific pAb or control rabbit IgG. Confocal images of frozen sections of duodenal PPs from naive BALB/c mice labeled with UEA-1-rhodamine, DAPI, and immune complexes of FITC-labeled anti-rabbit IgG secondary Ab with anti-MLP polyclonal Ab or normal rabbit IgG. *1* and *5*, Merged images of DAPI (blue) and MLP (green) (*1*) or normal rabbit IgG (green) (*5*). *2–4*, High magnification of a PP FAE. *2*, Merged image of DAPI-(blue) and MLP (green)-staining. *3*, Single image of UEA-1-staining (red). *4*, Merged image of (*2*) and (*3*). Arrows show PP M cells expressing MLP. Scale bar = 100 μm (*1*), 50 μm (*5*), and 10 μm (*2–4*).

Unique expression of chemokines in PP M cells and/or CT-induced villous M-like cells

Focusing on chemokines whose presence was statistically identified regardless of the raw value, we found seven chemokines to be expressed by PP M cells and/or CT-induced villous M-like cells (Table I). In addition to the previously reported CCL9 and CCL20 that are expressed by the M cell-containing PP FAE (13–15), we found significant expression of CXCL13 and chemokine-like factor (CKLF) in PP M cells. Although CT-induced villous M-like cells and IECs constitutively expressed CCL6 and CCL28, the expression level of these chemokines was highest in PP M cells (thereby categorized in Group G; Fig. 2, *B* and *C*). Next, we also examined the expression pattern of chemokines in CT-induced villous M-like cells, finding, as in PP M cells, an up-regulation of CCL9, CKLF, and CCL6 mRNAs. Their raw values and expression levels were higher than those seen in IECs (Table I). Furthermore, CT-induced villous M-like cells showed the highest expression of CXCL16 mRNA, with expression levels 1.9–2.5-fold higher than in PP M cells and 2.1–2.3-fold higher than in IECs (Table I).

Table I. *Chemokines expressed by PP M cells and/or CT-induced villous M-like cells*[a]

Name	GenBank	Affymetrix Probe No.	Group (see Fig. 2*C*)	Relative Expression Level against IEC	
				PP-M	Vi-M
CCL9	AF128196	1417936_at	A	124.8	7.0
CXCL13	AF030636	1417851_at	A	64.4	-
CKLF	BE852312	1436242_a_at	A	52.2	8.3
CCL6	AV084904	1420249_s_at	G	30.4	5.1
	BC002073	1417266_at	G	12.5	4.6
CCL20	AF099052	1422029_at	A	10.9	-
CCL28	BE196980	1455577_at	G	2.8	0.7
CXCL16	BC019961	1449195_s_at	G	1.1	2.1
		1418718_at	G	0.9	2.3

[a] Expression levels on probes identified as "Present Call" in PP M cells (PP-M) or CT-induced villous M-like cells (Vi-M) were compared with those in IECs. Minus indicated no expression in Vi-M and IECs. CKLF, Chemokine-like factor.

Discussion

In this study, we combined the advanced techniques of M cell purification and DNA microarrays to construct a gene-profiling database for PP M cells, CT-induced villous M-like cells, and IECs. The lack of M cell-specific markers has long presented an obstacle to the isolation of M cells. We overcame this barrier by using M cell-specific NKM 16-2-4 mAb. Our knowledge that villous M (or M-like) cells, usually low frequency in the duodenum, could be increased by CT allowed us to separately isolate PP M cells, CT-induced villous M-like cells, and IECs using FACS. Of course, we cannot yet exclude the possibility that individual cell-sorted fractions were mildly contaminated by other cell types; however, we regard the database as reliable because most of the previously reported PP M cell-specific genes encoding peptidoglycan recognition protein-S, secretory granule neuroendocrine protein 1, and annexin V (4–6) were found in the PP M cell-significant group (Group A). Thus, the gene-profiling database presented

here has several advantages: it appears reliable because it was capable of confirming already established findings; it includes villous M (or M-like) cells as well as PP M cells and IECs; and it is based on a purified cell population. These advantages could make this gene-profiling database a reliable and useful tool for identifying new molecules expressed by M cells and for deepening our understanding of M cell immunobiology.

A mucosal vaccine delivery system targeting PP M cells would be more effective at generating not only efficient mucosal but also systemic immunity. When UEA-1 was used as an Ag delivery vehicle, the administration of PP M cell-targeted Ags induced Ag-specific mucosal and systemic immune responses (16) despite the cospecificity of the lectin for M cells and goblet cells (3). The gene-profiling database was, therefore, used to look for candidate target molecules in the vaccine delivery system. We focused on GP2, which is a GPI-anchored protein expressed at a higher level in Group A. GP2 is associated with lipid rafts, is sorted to the apical plasma membrane (17), and is likely to possess a similar distribution in PP M cells. Additional mRNA and protein analyses by ISH and immunohistochemistry identified the specific expression of GP2 in the apical plasma membrane of PP M cells. Although the role played by GP2 in a unique Ag-sampling system of PP M cells remains obscure, GP2 is not required for PP M cell development, as evidenced by the presence of M cells in the FAE of PPs from *GP2*$^{-/-}$ mice (data not shown). Taken together, these findings support the candidacy of GP2 as an M cell-targeting molecule. If it is in fact confirmed to be so, it could greatly contribute to the development of a mucosal vaccine delivery system.

In addition to the identification of GP2, reliance of the gene-profiling database is further supported by the identification of specific expression of MLP by PP M cells. Not only *MLP* but also other genes have been previously reported as FAE-specific genes (5, 6). Using DNA microarray analysis, we were able to identify most such genes, including *MLP*, as PP M cell-significant genes. This study demonstrated for the first time the histological distribution of expressed MLP mRNA and protein in the small intestine. MLP, a member of protein kinase C substrates, binds calcium/calmodulin and actin (18, 19), and has been implicated in integrin-dependent phagocytosis by macrophages (20, 21). However, that contention was challenged in another study by Underhill and coworkers (22) using *MLP*$^{-/-}$ macrophages. Interestingly, β1 integrin, which is expressed by the apical membrane of PP M cells but not of IECs in the murine small intestine, is involved in the uptake of *Yersinia* by PP M cells via integrin-invasin binding (23). Thus, MLP may also account for the Ag uptake/sampling process, including integrin-dependent Ag uptake, of M cells located within the FAE of PPs.

Our constructed gene profiling also provides additional information for M cell immunobiology. Both PP and villous M cells contain in their basolateral region immunocompetent cells characterized by a pocket formation (3, 24), the contents of which are influenced by the repertoire of chemokines expressed by M cells. So far, three chemokines, CCL9, CCL20, and CXCL16, have been reported to be specifically expressed by the M cell-containing FAE of PPs and to contribute to the spatial distribution of dendritic cells or T cells in the subepithelial dome as well as in the basolateral pocket regions of M cells (13–15, 25). Our examination for the gene expression pattern of chemokines using the gene-profiling database showed that CXCL13, CKLF, CCL6, and CCL28, in addition to CCL9 and CCL20, are specifically or highly expressed by PP M cells, suggesting that CXCL13, CKLF, CCL6, and CCL28 may also play a role in regulating the recruitment of various immunocompetent cells into the pocket region of PP M cells.

Noticeably, CT-induced villous M-like cells share with PP M cells the expression of certain chemokines, including CCL6, CCL9, and CKLF. Furthermore, the highest expression of CXCL16 mRNA was observed in CT-induced villous M-like cells, although CXCL16 has previously been shown to be specifically expressed in the FAE of PPs (25). This discrepancy may result from our exclusive use of duodenal tissues for the analysis of M cell gene profiling. CXCL16 is a chemoattractant for activated CD8$^+$ T cells and, to a lesser extent, for activated CD4$^+$ T cells (25, 26); the CXCL16 receptor is expressed by intraepithelial lymphocytes (IELs) (26). In the small intestine, the distribution patterns for CD4$^+$ and CD8$^+$ T cells are distinct, with CD4$^+$ T cells primarily located in the lamina propria and CD8$^+$ T cells residing along the epithelium (27). When CT was orally administered, CD8$^+$ IELs were rapidly and transiently depleted (28). Interestingly, we observed that CD8$^+$ IEL numbers recovered following the generation of CT-induced villous M-like cells (data not shown). Therefore, our current finding that CT-induced villous M-like cells express a higher level of CXCL16 makes it plausible that CD8$^+$ T cells are retained in the intestinal epithelium, mainly into the pocket of villous M-like cells. Furthermore, up-regulation of CCL9, CKLF, CCL6, and CXCL16 in CT-induced villous M-like cells could account for the CT-induced recruitment of immunocompetent cells to the site of Ag sampling from the intestinal lumen via CT-induced villous M-like cells.

Although the development mechanism of villous M cells remains unclear, we hypothesize that villous M cells are differentiated from IECs by exogenous stimuli because oral CT administration resulted in the induction of villous M-like cells in the middle to upper regions of villi (Terahara et al., submitted for publication), i.e., where IECs normally migrate from the crypts to the villus (29). Our hypothesis is also informed by the suggestions offered by other groups that IECs in the FAE of PPs could be converted to M cells by bacterial infection and inflammation (30, 31). We propose that CT-induced villous M-like cells have a gene expression pattern that is intermediate between PP M cells and IECs, as evidenced by the very similar correlation coefficient values obtained when the comprehensive gene profile of CT-induced villous M-like cells was compared with that of PP M cells (r^2 = 0.402) and IECs (r^2 = 0.410). The intermediate nature of CT-induced villous M-like cells between PP M cells and IECs is further confirmed by chemokine expression profiles. In this study, we have attempted to use gene profiling to elucidate the development mechanism of villous M cells.

In conclusion, our gene-profiling database should prove a valuable tool in identifying suitable M cell-targeting molecules, thereby speeding the development of a mucosal vaccine delivery system as well as allowing for a better understanding of M cell immunobiology.

Acknowledgments

We thank the members of our laboratory for technical advice and helpful discussions. We also extend our thanks to Dr. K. McGhee for editorial help.

Disclosures

The authors have no financial conflict of interest.

References

1. Gebert, A., H. J. Rothkötter, and R. Pabst. 1996. M cells in Peyer's patches of the intestine. *Int. Rev. Cytol.* 167: 91–159.
2. Neutra, M. R., A. Frey, and J. P. Kraehenbuhl. 1996. Epithelial M cells: gateways for mucosal infection and immunization. *Cell* 86: 345–348.
3. Jang, M. H., M. N. Kweon, K. Iwatani, M. Yamamoto, K. Terahara, C. Sasakawa, T. Suzuki, T. Nochi, Y. Yokota, P. D. Rennert, et al. 2004. Intestinal villous M

cells: an antigen entry site in the mucosal epithelium. *Proc. Natl. Acad. Sci. USA* 101: 6110–6115.
4. Lo, D., W. Tynan, J. Dickerson, J. Mendy, H. W. Chang, M. Scharf, D. Byrne, D. Brayden, L. Higgins, C. Evans, and D. J. O'Mahony. 2003. Peptidoglycan recognition protein expression in mouse Peyer's patch follicle associated epithelium suggests functional specialization. *Cell. Immunol.* 224: 8–16.
5. Hase, K., S. Ohshima, K. Kawano, N. Hashimoto, K. Matsumoto, H. Saito, and H. Ohno. 2005. Distinct gene expression profiles characterized cellular phenotypes of follicle-associated epithelium and M cells. *DNA Res.* 12: 127–137.
6. Verbrugghe, P., W. Waelput, B. Dieriks, A. Waeytens, J. Vandesompele, and C. A. Cuvelier. 2006. Murine M cells express annexin V specifically. *J. Pathol.* 209: 240–249.
7. Clark, M. A., M. A. Jepson, N. L. Simmons, T. A. Booth, and B. H. Hirst. 1993. Differential expression of lectin-binding sites defines mouse intestinal M-cells. *J. Histochem. Cytochem.* 41: 1679–1687.
8. Nochi, T., Y. Yuki, A. Matsumura, M. Mejima, K. Terahara, D. Y. Kim, S. Fukuyama, K. Iwatsuki-Horimoto, Y. Kawaoka, T. Kohda, et al. 2007. A novel M-cell-specific carbohydrate-targeted mucosal vaccine effectively induces antigen-specific immune responses. *J. Exp. Med.* 204: 2789–2796.
9. Jackson, R. J., K. Fujihashi, J. Xu-Amano, H. Kiyono, C. O. Elson, and J. R. McGhee. 1993. Optimizing oral vaccines: induction of systemic and mucosal B-cell and antibody responses to tetanus toxoid by use of cholera toxin as an adjuvant. *Infect. Immun.* 61: 4272–4279.
10. Xu-Amano, J., H. Kiyono, R. J. Jackson, H. F. Staats, K. Fujihashi, P. D. Burrows, C. O. Elson, S. Pillai, and J. R. McGhee. 1993. Helper T cell subsets for immunoglobulin A responses: oral immunization with tetanus toxoid and cholera toxin as adjuvant selectively induces Th2 cells in mucosa associated tissues. *J. Exp. Med.* 178: 1309–1320.
11. Yamamoto, M., K. Fujihashi, K. Kawabata, J. R. McGhee, and H. Kiyono. 1998. A mucosal intranet: intestinal epithelial cells down-regulate intraepithelial, but not peripheral, T lymphocytes. *J. Immunol.* 160: 2188–2196.
12. Yoshida, S., K. Ohbo, A. Takakura, H. Takebayashi, T. Okada, K. Abe, and Y. Nabeshima. 2001. Sgn1, a basic helix-loop-helix transcription factor delineates the salivary gland duct cell lineage in mice. *Dev. Biol.* 240: 517–530.
13. Zhao, X., A. Sato, C. S. Dela Cruz, M. Linehan, A. Luegering, T. Kucharzik, A. K. Shirakawa, G. Marquez, J. M. Farber, I. Williams, and A. Iwasaki. 2003. CCL9 is secreted by the follicle-associated epithelium and recruits dome region Peyer's patch CD11b$^+$ dendritic cells. *J. Immunol.* 171: 2797–2803.
14. Iwasaki, A., and B. L. Kelsall. 2000. Localization of distinct Peyer's patch dendritic cell subsets and their recruitment by chemokines macrophage inflammatory protein (MIP)-3α, MIP-3β, and secondary lymphoid organ chemokine. *J. Exp. Med.* 191: 1381–1393.
15. Cook, D. N., D. M. Prosser, R. Forster, J. Zhang, N. A. Kuklin, S. J. Abbondanzo, X. D. Niu, S. C. Chen, D. J. Manfra, M. T. Wiekowski, et al. 2000. CCR6 mediates dendritic cell localization, lymphocyte homeostasis, and immune responses in mucosal tissue. *Immunity* 12: 495–503.
16. Wang, X., I. Kochetkova, A. Haddad, T. Hoyt, D. M. Hone, and D. W. Pascual. 2005. Transgene vaccination using *Ulex europaeus* agglutinin I (UEA-1) for targeted mucosal immunization against HIV-1 envelope. *Vaccine* 23: 3836–3842.
17. Mays, R. W., K. A. Siemers, B. A. Fritz, A. W. Lowe, G. van Meer, and W. J. Nelson. 1995. Hierarchy of mechanisms involved in generating Na/K-ATPase polarity in MDCK epithelial cells. *J. Cell Biol.* 130: 1105–1115.
18. Aderem, A. 1992. The MARCKS brothers: a family of protein kinase C substrates. *Cell* 71: 713–716.
19. Blackshear, P. J. 1993. The MARCKS family of cellular protein kinase C substrates. *J. Biol. Chem.* 268: 1501–1504.
20. Zhu, Z., Z. Bao, and J. Li. 1995. MacMARCKS mutation blocks macrophage phagocytosis of zymosan. *J. Biol. Chem.* 270: 17652–17655.
21. Li, J., Z. Zhu, and Z. Bao. 1996. Role of MacMARCKS in integrin-dependent macrophage spreading and tyrosine phosphorylation of paxillin. *J. Biol. Chem.* 271: 12985–12990.
22. Underhill, D. M., J. Chen, L. A. H. Allen, and A. Aderem. 1998. MacMARCKS is not essential for phagocytosis in macrophages. *J. Biol. Chem.* 273: 33619–33623.
23. Clark, M. A., B. H. Hirst, and M. A. Jepson. 1998. M-cell surface β1 integrin expression and invasin-mediated targeting of *Yersinia pseudotuberculosis* to mouse Peyer's patch M cells. *Infect. Immun.* 66: 1237–1243.
24. Owen, R. L., and A. L. Jones. 1974. Epithelial cell specialization within human Peyer's patches: an ultrastructural study of intestinal lymphoid follicles. *Gastroenterology* 66: 189–203.
25. Hase, K., T. Murakami, H. Takatsu, T. Shimaoka, M. Iimura, K. Hamura, K. Kawano, S. Ohshima, R. Chihara, K. Itoh, et al. 2006. The membrane-bound chemokine CXCL16 expressed on follicle-associated epithelium and M cells mediates lympho-epithelial interaction in GALT. *J. Immunol.* 176: 43–51.
26. Matloubian, M., A. David, S. Engel, J. E. Ryan, and J. G. Cyster. 2000. A transmembrane CXC chemokine is a ligand for HIV-coreceptor Bonzo. *Nat. Immunol.* 1: 298–304.
27. Jahnsen, F. L., I. N. Farstad, J. P. Aanesen, and P. Brandtzaeg. 1998. Phenotypic distribution of T cells in human nasal mucosa differs from that in the gut. *Am. J. Respir. Cell Mol. Biol.* 18: 392–401.
28. Flach, C. F., S. Lange, E. Jennische, I. Lönnroth, and J. Holmgren. 2005. Cholera toxin induces a transient depletion of CD8$^+$ intraepithelial lymphocytes in the rat small intestine as detected by microarray and immunohistochemistry. *Infect. Immun.* 73: 5595–5602.
29. Leblond, C. P., and B. Messier. 1958. Renewal of chief cells and goblet cells in the small intestine as shown by radioautography after injection of thymidine-H3 into mice. *Anat. Rec.* 132: 247–259.
30. Borghesi, C., M. J. Taussig, and C. Nicoletti. 1999. Rapid appearance of M cells after microbial challenge is restricted at the periphery of the follicle-associated epithelium of Peyer's patch. *Lab. Invest.* 79: 1393–1401.
31. Lügering, A., M. Floer, N. Lügering, C. Cichon, M. A. Schmidt, W. Domschke, and T. Kucharzik. 2004. Characterization of M cell formation and associated mononuclear cells during indomethacin-induced intestinal inflammation. *Clin. Exp. Immunol.* 136: 232–238.

INFECTION AND IMMUNITY, June 2008, p. 2777–2784 Vol. 76, No. 6
0019-9567/08/$08.00+0 doi:10.1128/IAI.01502-07

Nasal Vaccination with the 40-Kilodalton Outer Membrane Protein of *Porphyromonas gingivalis* and a Nontoxic Chimeric Enterotoxin Adjuvant Induces Long-Term Protective Immunity with Reduced Levels of Immunoglobulin E Antibodies▽

Fumiki Momoi,[1] Tomomi Hashizume,[1] Tomoko Kurita-Ochiai,[1] Yoshikazu Yuki,[2] Hiroshi Kiyono,[2] and Masafumi Yamamoto[1]*

Department of Microbiology and Immunology, Nihon University School of Dentistry at Matsudo, Chiba, Japan,[1] and Division of Mucosal Immunology, Department of Microbiology and Immunology, Institute of Medical Science, University of Tokyo, Tokyo, Japan[2]

Received 11 November 2007/Returned for modification 18 December 2007/Accepted 3 April 2008

In this study, we demonstrated that the 40-kDa outer membrane protein of *Porphyromonas gingivalis* (40-kDa OMP) nasally administered with a nontoxic chimeric adjuvant that combines the A subunit of mutant cholera toxin E112K with the pentameric B subunit of heat-labile enterotoxin from enterotoxigenic *Escherichia coli* (mCTA/LTB) elicited a long-term protective immune response. Immunization with the 40-kDa OMP and mCTA/LTB induced high levels of 40-kDa-OMP-specific immunoglobulin G (IgG) and IgA antibodies (Abs) in sera and elicited a significant IgA anti-40-kDa OMP Ab response in saliva. These Ab responses were maintained for at least 1 year after the immunization. Although using adjuvant mCTA/LTB gave Ab responses in the saliva comparable to those obtained using native cholera toxin (nCT) as the adjuvant, the levels of total IgE and 40-kDa-OMP-specific IgE Abs as well as interleukin-4 levels induced by the immunization with mCTA/LTB were lower than those induced by the immunization with nCT. Importantly, IgG Abs generated by nasal immunization with the 40-kDa OMP plus mCTA/LTB inhibited the coaggregation and hemagglutinin activities of *P. gingivalis*. Furthermore, the mice given nasal 40-kDa OMP plus mCTA/LTB showed a significant reduction of alveolar bone loss caused by oral infection with *P. gingivalis* even 1 year after the immunization compared to the loss in unimmunized mice. Because mCTA/LTB is nontoxic, nasally administered 40-kDa OMP together with mCTA/LTB should be an effective and safe mucosal vaccine against *P. gingivalis* infection in humans and may be an important tool for the prevention of chronic periodontitis.

Chronic periodontitis is a common oral inflammatory disease that causes the breakdown of periodontal tissue, including the resorption of alveolar bone, and as a consequence, tooth loss (8). Furthermore, recent studies have suggested that chronic periodontitis influences systemic conditions such as cardiovascular diseases, diabetes, and osteoporosis (5, 10, 19, 28, 39, 41, 45). Hence, the prevention of periodontitis is important for both oral and systemic health.

Porphyromonas gingivalis, a gram-negative anaerobic bacterium, has been shown previously to be one of the major pathogens in chronic periodontitis. The colonization of gingival tissues by this bacterium is considered to be the first step in the pathogenic process of periodontal disease resulting in tissue destruction (24, 37). Molecules such as fimbriae, hemagglutinins, aggregation factors, and lipopolysaccharides responsible for colonization have been identified previously as virulence factors (24, 37). An outer membrane protein having a molecular mass of 40 kDa produced by *P. gingivalis* (40-kDa OMP) is a key virulence factor involved in the coaggregation activity of *P. gingivalis* (23). Furthermore, this OMP has been shown previously to be a hemin-binding protein (49). The 40-kDa OMP resides both on the cell surface and in extracellular vesicles and is found on many strains of *P. gingivalis* (1, 22, 23, 47).

Previous studies have demonstrated that monoclonal antibodies (Abs) against the 40-kDa OMP provide an inhibitory effect on the coaggregation activity of *P. gingivalis* and possess complement-mediated bactericidal activity against *P. gingivalis* (23, 25, 46). Furthermore, human monoclonal Abs against the 40-kDa OMP provide protection against bone loss caused by *P. gingivalis* in rats (21). These studies suggest that the induction of 40-kDa-OMP-specific Abs in the oral mucosa is a logical approach for the prevention of *P. gingivalis* infection.

Cholera toxin (CT) and heat-labile enterotoxin (LT) from enterotoxigenic *Escherichia coli* are structurally similar, and both toxins act as adjuvants for the enhancement of mucosal and systemic Ab responses to coadministered protein antigen (Ag) given by mucosal routes (51, 58). Indeed, one of our previous studies demonstrated that the nasal administration of the 40-kDa OMP plus CT elicits 40-kDa-OMP-specific secretory immunoglobulin A (IgA) Abs in the saliva, as well as IgG Abs in serum, that inhibit the coaggregation activity of *P. gingivalis* (43). However, though the combination of the 40-kDa OMP with the adjuvant CT was shown to be effective, CT and LT cause severe diarrhea and thus are unsuitable for use in humans. Hence, nontoxic mutant derivatives of CT or LT have been generated previously for the development of safe adjuvants (9, 11, 13, 15, 18, 35).

* Corresponding author. Mailing address: Department of Microbiology and Immunology, Nihon University School of Dentistry at Matsudo, 2-870-1 Sakaecho-Nishi, Matsudo, Chiba 271-8587, Japan. Phone: 81-47-360-9336. Fax: 81-47-360-9601. E-mail: yamamoto.masafumi@nihon-u.ac.jp.

▽ Published ahead of print on 14 April 2008.

We generated mutant CTs (mCTs) by replacing a single amino acid in the ADP-ribosyltransferase active center of the A subunit. These newly created mCTs (S61F and E112K) do not induce enzymatic activity and cyclic AMP formation but still retain adjuvanticity (59, 60). Furthermore, we constructed a novel nontoxic chimeric mucosal adjuvant that combines the nontoxic A subunit of mCT E112K with the pentameric B subunit of LT from enterotoxigenic *E. coli* (mCTA/LTB). Interestingly, mCTA/LTB acts as a mucosal adjuvant and provides effective support for protective Ab responses against bacterial toxins and influenza virus infection (33).

In this study, we assessed the potential of a combined intranasal vaccine, the 40-kDa OMP with mCTA/LTB, to prevent oral infection with *P. gingivalis*. The results suggest that nasal 40-kDa OMP plus mCTA/LTB is a practical and effective vaccine candidate for the induction of protective immunity against alveolar bone loss caused by *P. gingivalis* infection.

MATERIALS AND METHODS

Mice. Female BALB/c Cr Slc (BALB/c) mice were purchased from Sankyo Laboratories and were maintained under specific-pathogen-free conditions at the experimental facility of the Nihon University School of Dentistry at Matsudo, Chiba, Japan. Mice received sterile food and water and were 8 to 12 weeks old when used for experiments. All animals were maintained and used in accordance with the guidelines for the care and use of laboratory animals of the Nihon University School of Dentistry at Matsudo.

Ag and adjuvants. Plasmid pMD125 expressing the 40-kDa OMP was kindly provided by Yoshimitsu Abiko (Nihon University). The 40-kDa OMP was purified to homogeneity from a suspension of *E. coli* K-12 cells harboring pMD125, as described previously (26). The purity of the 40-kDa OMP was determined by sodium dodecyl sulfate-polyacrylamide gel electrophoresis, and no contaminating protein bands were noted. Furthermore, the possible presence of residual endotoxin in the preparation was assessed with a *Limulus* amoebocyte lysate pyrochrome kit (Associates of Cape Cod Inc., Woods Hole, MA). The 40-kDa-OMP preparation contained as little as 0.4 pg of endotoxin.

A plasmid containing both E112K mCTA and LTB genes (pNCMO2-LTB-mCTA) was constructed as described previously (33). *E. coli* JM109 (Takara Bio Inc., Shiga, Japan) was used as a cloning host, and *Brevibacillus choshinensis* HPD31 was used as the host for the production of the recombinant protein (42). The mCTA/LTB chimeric protein was purified from culture supernatants of transformants containing pNCMO2-LTB-mCTA. Purity was examined by sodium dodecyl sulfate-polyacrylamide gel electrophoresis. The protein concentration was determined by using MicroBCA protein assay reagent (Pierce). CT was obtained from List Biologic Laboratories (Campbell, CA).

Immunization and sample collection. Mice were immunized nasally on days 0, 7, and 14 with 20-μl aliquots (10 μl per nostril) of phosphate-buffered saline (PBS) containing 10 μg of the 40-kDa OMP alone or combined with 10 μg of mCTA/LTB or 1 μg of native CT (nCT). Serum and saliva samples were collected from each group, as described elsewhere (56), in order to examine 40-kDa-OMP-specific Ab responses.

Detection of Ag-specific Ab response. Ab titers in serum and saliva samples were determined by an enzyme-linked immunosorbent assay (ELISA) (38, 53). Briefly, plates were coated with the 40-kDa OMP (5 μg/ml) and blocked with 1% bovine serum albumin (BSA), and analyses were performed in duplicate. After the plates were blocked, serial dilutions of serum or saliva samples were added in duplicate. Starting dilutions of serum and saliva samples were $1:2^5$ and $1:2^2$, respectively. Following incubation, plates were washed and peroxidase-labeled goat anti-mouse γ- or α-heavy-chain-specific Abs (Southern Biotechnology Associates, Birmingham, AL) were added to appropriate wells. Finally, 2,2'-azino-bis(3-ethylbenz-thiazoline-6-sulfonic acid) with H_2O_2 (Moss, Inc, Pasadena, MD) was added for color development. End point titers were expressed as the $\log_2$ reciprocal of the last dilution giving an optical density at 414 nm of 0.1 greater than the background level after 15 min of incubation.

Analysis of 40-kDa-OMP-specific IgE Abs in sera. For the detection of 40-kDa-OMP-specific IgE Ab levels in sera, immunoplates (Nunc, Inc., Naperville, IL) were coated with purified rat anti-mouse IgE monoclonal Ab (BD Biosciences, San Diego, CA) and incubated overnight at 4°C, as described previously (32). After blocking of the plates with 3% BSA in PBS, serial dilutions of serum samples were added and the plates were incubated for 4 h at room temperature. Following extensive washing, 40-kDa OMP that had been biotinylated by using a biotin-labeling kit (Boehringer Ingelheim) was added. After the plates were incubated overnight at 4°C, peroxidase-labeled antibiotin monoclonal Abs (Vector Laboratories, Burlingame, CA) were added. After the plates were washed, the color reaction was developed with 3,3',5,5'-tetramethyl-benzidine (Moss) and stopped with 0.5 N HCl. End point titers of 40-kDa-OMP-specific IgE were expressed as the $\log_2$ reciprocal as described above.

Analysis of IL-4 response in 40-kDa-OMP-specific CD4$^+$ T cells. CD4$^+$ T cells from spleens were purified using a magnet-activated cell sorter system (Miltenyi Biotec, Auburn, CA), as described elsewhere (56). Purified CD4$^+$ T cells (2.5×10^6 cells/ml) were cultured with 2 μg of the 40-kDa OMP/ml in the presence of T-cell-depleted, mitomycin-treated splenic feeder cells (2.5×10^6 cells) in RPMI 1640 medium (GIBCO BRL, Rockville, MD) containing 10% fetal bovine serum, 50 μM 2-mercaptoethanol, 15 mM HEPES, 2 mM L-glutamine, 100 U of penicillin/ml, 100 μg of streptomycin/ml, and 10 U of recombinant IL-2 (Genzyme, Cambridge, MA)/ml. Cultures were incubated for 5 days at 37°C under 5% CO_2 in air. Levels of interleukin-4 (IL-4) in culture supernatants were determined by an IL-4-specific ELISA, as described previously (53). Briefly, 96-well plates (Nunc) were coated with a monoclonal anti-IL-4 Ab (BD Biosciences). After the plates were blocked with PBS containing 1% BSA, samples were added to duplicate wells and the plates were incubated overnight at 4°C. Wells were washed and incubated with biotinylated monoclonal anti-IL-4 Ab (BD Biosciences). After incubation, horseradish peroxidase-labeled antibiotin Ab (Vector Laboratories) was added and the reaction was developed with 3,3',5,5'-tetramethyl-benzidine (Moss) and stopped with 0.5 N HCl. Standard curves were generated using mouse recombinant IL-4 (Endogen, Boston, MA).

Coaggregation assay. IgG Abs in sera from immunized mice were purified using a HiTrap protein G HP column (Amersham Biosciences, Piscataway, MJ). *P. gingivalis* 381 and *Streptococcus gordonii* Challis were grown in a brain heart infusion (BBL Microbiology Systems, Cockeysville, MD) containing yeast extract (0.25%), hemin (10 μg/ml), and vitamin K (1 μg/ml). Bacterial cells were incubated at 37°C in an anaerobic chamber containing N_2 (80%), H_2 (10%), and CO_2 (10%). Coaggregation was determined by the visual assay method, as described previously (14, 36). Briefly, *P. gingivalis* 381 cells (approximately 10^{10} cells/ml) were preincubated with purified IgG Abs at 37°C for 1 h. A *P. gingivalis* suspension (100 μl) was then mixed with an equal volume of an *S. gordonii* suspension (approximately 10^{10} cells/ml) on the flocculation slide. This mixture was subsequently incubated at 37°C for 10 min with rotation.

Hemagglutination assay. The hemagglutinating activity of *P. gingivalis* was assayed as described previously (50) by using mice erythrocytes. Briefly, *P. gingivalis* 381 cells were preincubated with purified IgG Abs at 37°C for 1 h. Fifty microliters of a *P. gingivalis* cell suspension (0.5 μg) in PBS was transferred into microtiter wells, and 50 μl of 1% mice erythrocytes was added. After incubation for 1 h at 37°C with humidity, the hemagglutinating activity of *P. gingivalis* was observed.

Oral infection. Mice were orally infected with *P. gingivalis* as described previously (3, 17, 34) with minor modifications. Briefly, mice were given sulfamethoxazole-trimethoprim (Sulfatrim; Goldline Laboratories, Ft. Lauderdale, FL) at 10 ml per pint in deionized water ad libitum for 10 days. This treatment was followed by a 3-day antibiotic-free period. Mice were then given 10^9 CFU of *P. gingivalis* suspended in 100 μl of PBS with 2% carboxymethylcellulose via oral topical application over 3 weeks for a total 15 inoculations. Control groups included mock-infected mice, which received the antibiotic pretreatment and carboxymethylcellulose without *P. gingivalis*. Forty-seven days after the first gavage, mice were euthanized using CO_2.

Measurement of alveolar bone loss. Horizontal bone loss around the maxillary molars was assessed by a morphometric method as described previously (29). Briefly, skulls were unfleshed after 10 min of treatment in boiling water under pressure of 15 lb/in^2, immersed overnight in 3% hydrogen peroxide, pulsed for 1 min in bleach, and stained with 1% methylene blue. The distance from the cementoenamel junction to the alveolar bone crest was measured at a total of 14 buccal sites per mouse. Measurements were made under a dissecting microscope (magnification, ×50) fitted with a video image marker measurement system (VHX-100; KEYENCE, Osaka, Japan) standardized to give measurements in micrometers. Bone measurements were performed a total of three times by two evaluators using a random and blind protocol.

Statistics. Data are expressed as means ± standard errors (SE) and were compared using an unpaired Student *t* test.

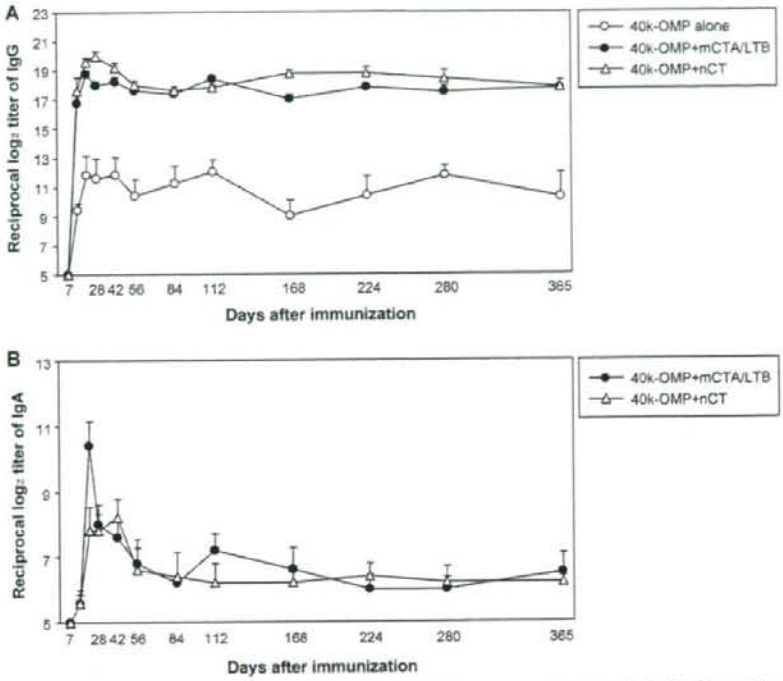

FIG. 1. 40-kDa-OMP-specific IgG and IgA Ab responses in sera. Groups of mice were nasally immunized with 10 μg of the 40-kDa OMP alone, 10 μg of the 40-kDa OMP plus 10 μg of mCTA/LTB, or 10 μg of the 40-kDa OMP plus 1 μg of nCT on days 0, 7, and 14. Serum samples were assessed for 40-kDa-OMP-specific IgG (A) and IgA (B) Abs. Results are expressed as the means ± standard errors (SE) for four mice per group and a total of three experiments. IgA anti-40-kDa OMP Abs in sera from mice given the 40-kDa OMP alone were not detectable throughout the experimental period. The *P* values for IgG and IgA Ab titers obtained with the 40-kDa OMP plus mCTA/LTB or the 40-kDa OMP plus nCT compared to those obtained with the 40-kDa OMP alone at all times except day 7 are <0.05.

RESULTS

Nasal 40-kDa OMP with mCTA/LTB elicits long-term Ab responses. In the initial study, we sought to determine whether the nasal administration of the 40-kDa OMP with mCTA/LTB as a mucosal adjuvant could induce a 40-kDa-OMP-specific Ab response. Mice nasally immunized with the 40-kDa OMP plus mCTA/LTB showed significant 40-kDa-OMP-specific IgG and IgA Ab responses in sera that were comparable to those induced by the 40-kDa OMP plus nCT (Fig. 1). In contrast, only low levels of IgG Abs were induced after immunization with the 40-kDa OMP alone (Fig. 1A). In addition, the nasal administration of the 40-kDa OMP alone failed to elicit a 40-kDa-OMP-specific IgA Ab response detectable in the starting serum dilution ($\log_2$ of 5) used in these experiments. Importantly, the serum IgG and IgA Ab responses induced by the 40-kDa OMP plus mCTA/LTB or nCT persisted for more than 1 year (Fig. 1).

Nasal 40-kDa OMP plus mCTA/LTB induced high levels of 40-kDa-OMP-specific IgA Abs in saliva, and these Abs were maintained for more than 1 year, although the responses gradually decreased from day 28 (Fig. 2). In contrast, no such IgA Ab response was detected in mice given the 40-kDa OMP alone (IgA Ab titers, <$\log_2$ of 2). These serum IgG and IgA

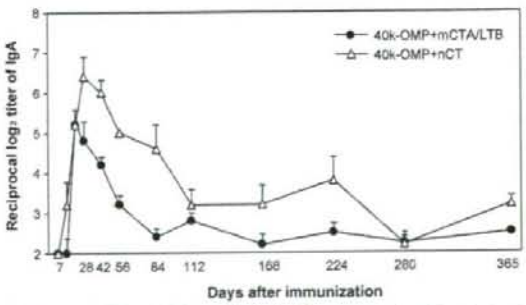

FIG. 2. 40-kDa-OMP-specific IgA Ab responses in saliva. Groups of mice were nasally immunized with the 40-kDa OMP plus mCTA/LTB or the 40-kDa OMP plus nCT as described in the legend to Fig. 1. Saliva samples were assessed for 40-kDa-OMP-specific IgA Abs. Results are expressed as the means ± SE for four mice per group and a total of three experiments. IgA anti-40-kDa OMP Abs in mice given the 40-kDa OMP alone were not detectable throughout the experimental period. The *P* values for Ab titers obtained with the 40-kDa OMP plus mCTA/LTB or the 40-kDa OMP plus nCT compared to those obtained with the 40-kDa OMP alone at all times except days 7 and 14 are <0.05.

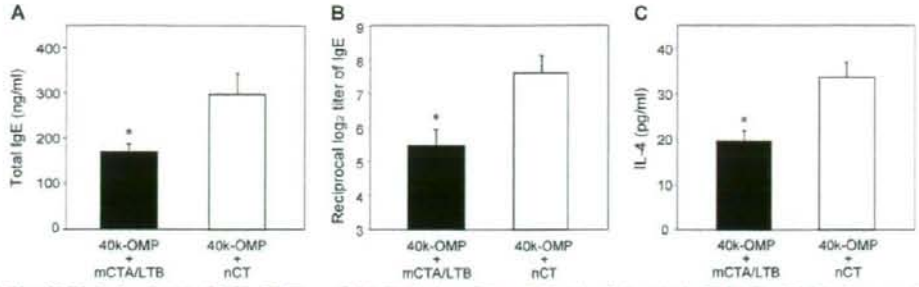

FIG. 3. Total IgE Ab levels (A), 40-kDa-OMP-specific IgE Ab titers (B), and IL-4 levels in splenic $CD4^+$ T cells (C). Groups of mice were nasally immunized with the 40-kDa OMP plus mCTA/LTB or the 40-kDa OMP plus nCT as described in the legend to Fig. 1. Seven days after the final immunization, serum samples were collected and assessed for total and 40-kDa-OMP-specific IgE Abs. For the measurement of IL-4 production, $CD4^+$ T cells obtained from the spleens of immunized mice were restimulated with the 40-kDa OMP. Culture supernatants were harvested, and the levels of secreted cytokines were assessed by a cytokine-specific ELISA. Results are expressed as the means ± SE for four mice per group and a total of three experiments. *, $P < 0.05$ compared with results for mice given the 40-kDa OMP plus nCT.

and salivary IgA Ab titers were confirmed by Ab-forming cell (AFC) responses, which indicated significant numbers of 40-kDa-OMP-specific IgG and IgA AFCs in the spleens, cervical lymph nodes, and submandibular glands of mice given the 40-kDa OMP plus mCTA/LTB or nCT, while low numbers of AFCs were detected in these tissues in mice given the 40-kDa OMP alone (data not shown). These results indicate that a combination of the 40-kDa OMP with mCTA/LTB is a potential nasal vaccine for the induction of Ag-specific mucosal and systemic Ab responses.

40-kDa-OMP-specific IL-4 and IgE Ab responses. Because mCTA/LTB given nasally has been shown previously to induce a weaker IgE Ab response than nCT (33), it is important to examine the IgE Ab response induced by the 40-kDa OMP together with mCTA/LTB. As may be expected, nasal immunization with the 40-kDa OMP plus nCT induced high-level total and 40-kDa-OMP-specific IgE Ab responses. In contrast, significantly lower levels of total and 40-kDa-OMP-specific IgE Abs in mice given the 40-kDa OMP plus mCTA/LTB than in mice given the 40-kDa OMP plus nCT were noted (Fig. 3A and B). An analysis of the IL-4 response confirmed the IgE Ab titers and showed that $CD4^+$ T cells from the spleens of mice immunized with the 40-kDa OMP plus mCTA/LTB, when restimulated with the 40-kDa OMP in vitro, produced significantly lower levels of IL-4 than those from mice immunized with the 40-kDa OMP plus nCT (Fig. 3B). These findings show that levels of 40-kDa-OMP-specific IL-4 and the subsequent IgE Ab response induced by the 40-kDa OMP plus mCTA/LTB were much lower than those evoked by the 40-kDa OMP plus nCT.

Nasally induced 40-kDa-OMP-specific IgG inhibits the coaggregation and hemagglutinin activities of *P. gingivalis*. We next determined whether the Abs induced by nasally administered 40-kDa OMP plus mCTA/LTB were capable of inhibiting the coaggregation and hemagglutinin activities of *P. gingivalis*. A flocculation slide assay showed that the coaggregation activity of *P. gingivalis* cells with *S. gordonii* cells was inhibited by IgG Abs from mice given the 40-kDa OMP plus mCTA/LTB in a dose-dependent manner. In contrast, IgG from mice given the 40-kDa OMP alone showed marginal effects against the coaggregation activity of *P. gingivalis* (Fig. 4A).

In the next study, the inhibitory effects of Abs induced by the 40-kDa OMP plus mCTA/LTB on the hemagglutinin activity of *P. gingivalis* were determined. IgG Abs purified from mice immunized with the 40-kDa OMP plus mCTA/LTB significantly inhibited the hemagglutinating activity of *P. gingivalis* in a dose-dependent manner. In contrast, although IgG from mice given the 40-kDa OMP alone showed some inhibition, the effects were much weaker than those of IgG from mice given the 40-kDa OMP with mCTA/LTB. As expected, IgG from unimmunized mice failed to inhibit the hemagglutinating activity of *P. gingivalis* (Fig. 4B).

Nasal 40-kDa OMP plus mCTA/LTB reduces alveolar bone loss caused by oral infection with *P. gingivalis*. As nasal 40-kDa OMP plus mCTA/LTB elicited long-term Ag-specific Ab responses in sera and saliva, we sought to determine whether these Abs were capable of suppressing bone resorption caused by oral infection with *P. gingivalis*. Thus, mice given the 40-kDa OMP plus mCTA/LTB or the 40-kDa OMP alone were infected orally with *P. gingivalis* 381 7 days or 1 year after immunization. Mice immunized with the 40-kDa OMP plus mCTA/LTB showed a significant reduction in alveolar bone loss caused by *P. gingivalis* infection 7 days after immunization compared to the loss in unimmunized mice (Fig. 5A and C). Furthermore, the Ag-specific Ab response induced by nasal 40-kDa OMP plus mCTA/LTB provided significant protection and reduced bone loss caused by *P. gingivalis* infection, even at 1 year after immunization (Fig. 5B and D). In contrast, mice immunized with the 40-kDa OMP alone did not exhibit reduced bone loss caused by *P. gingivalis* infection compared to that in unimmunized mice (Fig. 5). These findings indicate that nasal immunization with the 40-kDa OMP plus mCTA/LTB provides long-term protection against oral infection with *P. gingivalis*.

DISCUSSION

In this study, we demonstrated that the nasal administration of the 40-kDa OMP together with mCTA/LTB induced long-term 40-kDa-OMP-specific IgG and IgA in sera, as well as salivary IgA Abs, that persisted for more than 1 year. Furthermore, these mucosally induced IgG Abs inhibited the coaggre-

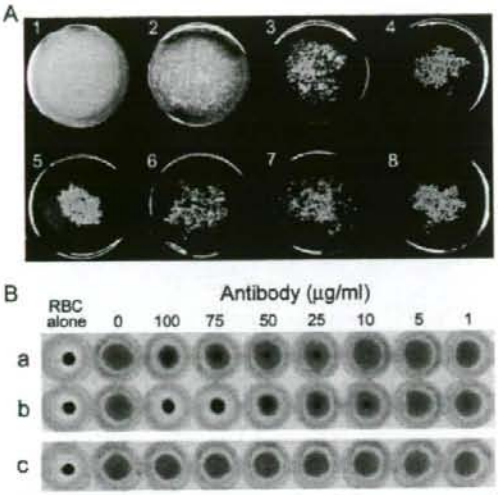

FIG. 4. Effects of 40-kDa-OMP-specific IgG Abs on coaggregation activity and hemagglutinin activity of *P. gingivalis*. (A) *P. gingivalis* was preincubated with 40-kDa-OMP-specific IgG and then mixed with *S. gordonii* on the flocculation slide for the assessment of coaggregation activity. Results of the flocculation slide assay with *S. gordonii* (panel 1), a mixture of *S. gordonii* and *P. gingivalis* with 150-μg/ml IgG Abs derived from the sera of mice given the 40-kDa OMP plus mCTA/LTB (panel 2), a mixture of *S. gordonii* and *P. gingivalis* with 100-μg/ml IgG Abs derived from the sera of mice given the 40-kDa OMP plus mCTA/LTB (panel 3), a mixture of *S. gordonii* and *P. gingivalis* with 50-μg/ml IgG Abs derived from the sera of mice given the 40-kDa OMP plus mCTA/LTB (panel 4), a mixture of *S. gordonii* and *P. gingivalis* (panel 5), a mixture of *S. gordonii* and *P. gingivalis* with 150-μg/ml IgG Abs derived from the sera of mice given the 40-kDa OMP alone (panel 6), a mixture of *S. gordonii* and *P. gingivalis* with 100-μg/ml IgG Abs derived from the sera of mice given the 40-kDa OMP alone (panel 7), and a mixture of *S. gordonii* and *P. gingivalis* with 50-μg/ml IgG Abs derived from the sera of mice given the 40-kDa OMP alone (panel 8) are shown. (B) For the hemagglutination assay, *P. gingivalis* was preincubated with several concentrations of 40-kDa-OMP-specific IgG Abs and then mixed with erythrocytes. Results of the hemagglutination assay with a mixture of erythrocytes and *P. gingivalis* with IgG Abs derived from the sera of mice given the 40-kDa OMP alone (row a), a mixture of erythrocytes and *P. gingivalis* with IgG Abs derived from the sera of mice given the 40-kDa OMP plus mCTA/LTB (row b), and a mixture of erythrocytes and *P. gingivalis* with IgG Abs derived from the sera of unimmunized mice (row c) are shown. IgG Abs used in this experiment were purified from the pooled sera of five mice per group. The results are representative of three separate experiments. RBC, red blood cells.

gation and hemagglutinin activities of *P. gingivalis*. Importantly, mice given the 40-kDa OMP plus mCTA/LTB were significantly protected against alveolar bone loss caused by oral infection with *P. gingivalis*, even 1 year after immunization. In the infection study, bone loss measured 1 year after immunization was greater than that measured 7 days after immunization, even in the absence of infection. In this regard, several studies have demonstrated a positive correlation between aging and alveolar bone loss (2, 4, 40). Another study using senescence-accelerated mice has demonstrated that alveolar bone loss is gradually increased with advancing age, although the mice do not develop chronic periodontitis (48). Thus, bone loss in the aged mice may be related to the aging process and to functional changes in tooth movement associated with aging. Taken together, these findings indicate that the 40-kDa OMP is an effective Ag for the induction of protective immune responses against *P. gingivalis* infection; however, mucosal immunization with the 40-kDa OMP alone induced only low levels of IgG anti-40-kDa OMP Abs in sera. IgA Abs were not detected in either serum or saliva samples. Indeed, the 40-kDa OMP without an adjuvant is a weak immunogen when given via the nasal route (43). Our previous studies have demonstrated that transcutaneous administration of the 40-kDa OMP without an adjuvant elicits a substantial IgG but not IgA Ab response in the sera and saliva of mice (36) and rats (30). However, transcutaneous immunization with the 40-kDa OMP alone failed to provide protection against bone loss caused by oral infection with *P. gingivalis* (unpublished observation). The findings of these studies together with our results in the present study indicate that mucosal adjuvants such as mCTA/LTB are required for the induction of the protective immune responses against oral infection with *P. gingivalis* when the 40-kDa OMP is given by mucosal routes.

CT and LT have been used widely as adjuvants for mucosal immunization, and our results indicate that the nasal administration of nCT with the 40-kDa OMP has an adjuvant effect and induces 40-kDa-OMP-specific mucosal IgA, as well as IgG and IgA Abs in serum (43). However, despite these beneficial attributes, CT and LT are unsuitable for use in humans because they cause severe diarrhea (51). To establish molecules that are nontoxic but retain adjuvant activity, several groups, including ours, have developed nontoxic mutant derivatives of CT or LT that may be suitable for use in humans (9, 11–13, 15, 18, 35, 44, 60). We previously showed that mCTA/LTB does not induce increases in intracellular cyclic AMP and fails to elicit fluid accumulation in ligated ileal loops (33). Furthermore, the nasal administration of an influenza vaccine together with the adjuvant mCTA/LTB elicits significant Ag-specific IgG and IgA Abs in the lung and provides complete protection against mucosal infection with influenza virus (33). The results of these studies demonstrate that mCTA/LTB is an effective adjuvant for nasal immunization and that, when given with the 40-kDa OMP, it facilitates the development of a long-term protective Ab response to the 40-kDa OMP. These results are the first to show that a nontoxic chimeric molecule combining the E112K mCTA and LTB induces a long-term protective Ab response to coadministered 40-kDa OMP in both serum and mucosal secretions.

As a mucosal adjuvant, CT given via mucosal routes induces Th2 cells that secrete high levels of IL-4 (55, 57, 58); however, the IL-4 cytokine provides a helper signal for the induction of IgE Abs that may cause anaphylactic reactions (27, 38). In this regard, our previous study demonstrated that biased Th1 and Th2 responses depend on the presence of the LT B subunit or the CT B subunit and that the CTA/LTB chimera, similar to LT, induces a gamma interferon- and IL-4-independent Th2 response while the chimera comprising the LT A subunit and the CT B subunit, similar to CT, elicits high-level IL-4 production along with an IgE Ab response (6). These results suggest that the B subunits of enterotoxins regulate T helper responses and that mCTA/LTB induces a low-level IL-4 response with subsequently reduced IgE Abs compared to those induced by

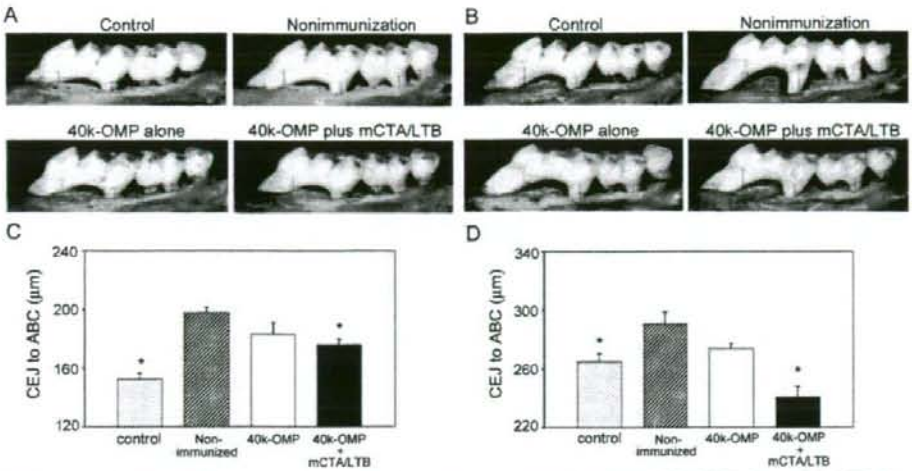

FIG. 5. Reduction of *P. gingivalis*-induced alveolar bone loss by a nasal vaccine containing the 40-kDa OMP plus mCTA/LTB. Groups of mice were immunized nasally with the 40-kDa OMP plus mCTA/LTB, the 40-kDa OMP alone, or PBS as described in the legend to Fig. 1. Seven days (A and C) or 1 year (B and D) after immunization, mice given PBS (unimmunized mice), the 40-kDa OMP alone, or the 40-kDa OMP plus mCTA/LTB were inoculated orally with 10^9 CFU of *P. gingivalis* in 2% carboxymethylcellulose, as described in Materials and Methods. Control mice were mock-infected mice inoculated with 2% carboxymethylcellulose only. The distances from the cementoenamel junction (CEJ) to the alveolar bone crest (ABC) at 14 predetermined sites in the unfleshed maxilla were measured and totaled for each mouse. Results are expressed as the means ± SE for six mice per group. *, $P < 0.05$ compared with results for unimmunized mice.

the LT A subunit/CT B subunit chimera. Indeed, in a previous study, the nasal administration of tetanus toxoid together with chimeric mCTA/LTB induced a marginal IgE Ab response (33). The results of this study also showed that nasal 40-kDa OMP plus mCTA/LTB induced significantly weaker 40-kDa-OMP-specific IL-4 and IgE Ab responses than the 40-kDa OMP plus nCT. Taken together with the present results, these data suggest that the mCTA/LTB chimera has the beneficial features of both enterotoxins and avoids the danger of allergic reactions provoked by IgE Abs.

The immunization protocol used in this study was designed to induce a significant 40-kDa-OMP-specific Ab response in the oral cavity. We selected nasal administration as the delivery route because of its successful record (6, 9, 12, 13, 18, 43, 56–59). However, nasally administered CT accumulates in the olfactory nerves and epithelial regions via GM-1 ganglioside (54). When used as a mucosal adjuvant, CT can influence the trafficking of coadministered protein Ag into these neuronal tissues (54). These findings raise some concerns about nasal administration and the potential threat posed by GM-1-binding molecules targeting neural tissues, including the central nervous system. However, another study has demonstrated that the deposition of CT in the olfactory tissues does not lead to obvious pathological changes in the brain after nasal administration (20). Although the exact effects of a nasally administered enterotoxin adjuvant on the central nervous system remain uncertain, a previous study has demonstrated that, unlike nCT, mCTA/LTB does not influence the trafficking of coadministered protein into the olfactory nerves and epithelium or into olfactory bulbs while mCTA/LTB itself accumulates in olfactory central nervous system regions (31). Taken together, these results suggest that mCTA/LTB is a more promising mucosal adjuvant than nCT.

The present results indicated that 40-kDa-OMP-specific IgG Abs inhibited the coaggregation and hemagglutinin activities of *P. gingivalis*. In this regard, it is known that immune responses in the oral cavity are derived from both the mucosal and systemic immune systems. The salivary glands, part of the mucosal immune system, are known to produce secretory IgA Abs in saliva. On the other hand, serum-derived IgG Ab-rich crevicular fluid, which continuously flows from the gingival capillaries, is part of the systemic immune system (7). Because *P. gingivalis* colonizes subgingival and supragingival biofilms (16, 31, 52), the generation of serum-derived IgG Abs in crevicular fluid, in addition to the IgA Ab response in saliva, may be effective in preventing *P. gingivalis* colonization.

In summary, this study has provided evidence that the nasal administration of the 40-kDa OMP together with nontoxic mCTA/LTB elicits 40-kDa-OMP-specific IgG and IgA in serum, as well as mucosal IgA Ab responses in saliva. These Ab responses persisted for more than 1 year after immunization. Moreover, 40-kDa-OMP-specific immune responses induced by the 40-kDa OMP plus mCTA/LTB provided protective immunity against alveolar bone loss caused by *P. gingivalis* infection. These findings suggest that nasally administered 40-kDa OMP with mCTA/LTB effectively elicits protective levels of Abs against the 40-kDa OMP and should therefore be considered as a candidate vaccine to immunize humans against *P. gingivalis* infection.

ACKNOWLEDGMENTS

This work was supported by grants-in-aid for scientific research (18592270, 19791624, and 19390537) from the Japan Society for the Promotion of Science and an "Academic Frontier" Project for Private Universities matching-fund subsidy from the Ministry of Education, Culture, Sports, Science and Technology, 2007 to 2011.

REFERENCES

1. **Abiko, Y., N. Ogura, U. Matsuda, K. Yanagi, and H. Takiguchi.** 1997. A human monoclonal antibody which inhibits the coaggregation activity of *Porphyromonas gingivalis*. Infect. Immun. **65:**3966–3969.
2. **Amstad-Jossi, M., and H. E. Schroeder.** 1978. Age-related alterations of periodontal structures around the cemento-enamel junction and of the gingival connective tissue composition in germ-free rats. J. Periodontal Res. **13:**76–90.
3. **Baker, P. J., R. T. Evans, and D. C. Roopenian.** 1994. Oral infection with *Porphyromonas gingivalis* and induced alveolar bone loss in immunocompetent and severe combined immunodeficient mice. Arch. Oral Biol. **39:**1035–1040.
4. **Barnett, N. A., and D. J. Rowe.** 1986. A comparison of alveolar bone in young and aged mice. J. Periodontol. **57:**447–452.
5. **Beck, J., R. Garcia, G. Heiss, P. S. Vokonas, and S. Offenbacher.** 1996. Periodontal disease and cardiovascular disease. J. Periodontol. **67:**1123–1137.
6. **Boyaka, P. N., M. Ohmura, K. Fujihashi, T. Koga, M. Yamamoto, M. N. Kweon, Y. Takeda, R. J. Jackson, H. Kiyono, Y. Yuki, and J. R. McGhee.** 2003. Chimeras of labile toxin one and cholera toxin retain mucosal adjuvanticity and direct Th cell subsets via their B subunit. J. Immunol. **170:**454–462.
7. **Challacombe, S. J., and P. J. Shirlaw.** 1999. Immunity of diseases of the oral cavity, p. 1313–1337. *In* P. L. Ogra, J. Mestecky, M. E. Lamm, W. Strober, J. Bienenstock, and J. R. McGhee (ed.), Mucosal immunology. Academic Press, San Diego, CA.
8. **Cutler, C. W., J. R. Kalmar, and C. A. Genco.** 1995. Pathogenic strategies of the oral anaerobe, Porphyromonas gingivalis. Trends Microbiol. **3:**45–51.
9. **de Haan, L., W. R. Verweij, I. K. Feil, T. H. Lijnema, W. G. Hol, E. Agsteribbe, and J. Wilschut.** 1996. Mutants of the *Escherichia coli* heat-labile enterotoxin with reduced ADP-ribosylation activity or no activity retain the immunogenic properties of the native holotoxin. Infect. Immun. **64:**5413–5416.
10. **DeStefano, F., R. F. Anda, H. S. Kahn, D. F. Williamson, and C. M. Russell.** 1993. Dental disease and risk of coronary heart disease and mortality. BMJ **306:**688–691.
11. **Dickinson, B. L., and J. D. Clements.** 1995. Dissociation of *Escherichia coli* heat-labile enterotoxin adjuvanticity from ADP-ribosyltransferase activity. Infect. Immun. **63:**1617–1623.
12. **Di Tommaso, A., G. Saletti, M. Pizza, R. Rappuoli, G. Dougan, S. Abrignani, G. Douce, and M. T. De Magistris.** 1996. Induction of antigen-specific antibodies in vaginal secretions by using a nontoxic mutant of heat-labile enterotoxin as a mucosal adjuvant. Infect. Immun. **64:**974–979.
13. **Douce, G., C. Turcotte, I. Cropley, M. Roberts, M. Pizza, M. Domenghini, R. Rappuoli, and G. Dougan.** 1995. Mutants of *Escherichia coli* heat-labile toxin lacking ADP-ribosyltransferase activity act as nontoxic, mucosal adjuvants. Proc. Natl. Acad. Sci. USA **92:**1644–1648.
14. **Ellen, R. P., and D. A. Grove.** 1989. *Bacteroides gingivalis* vesicles bind to and aggregate *Actinomyces viscosus*. Infect. Immun. **57:**1618–1620.
15. **Fontana, M. R., R. Manetti, V. Giannelli, C. Magagnoli, A. Marchini, R. Olivieri, M. Domenighini, R. Rappuoli, and M. Pizza.** 1995. Construction of nontoxic derivatives of cholera toxin and characterization of the immunological response against the A subunit. Infect. Immun. **63:**2356–2360.
16. **Gibbons, R. J., and M. Nygaard.** 1970. Interbacterial aggregation of plaque bacteria. Arch. Oral Biol. **15:**1397–1400.
17. **Gibson, F. C., III, C. Hong, H. H. Chou, H. Yumoto, J. Chen, E. Lien, J. Wong, and C. A. Genco.** 2004. Innate immune recognition of invasive bacteria accelerates atherosclerosis in apolipoprotein E-deficient mice. Circulation **109:**2801–2806.
18. **Giuliani, M. M., G. Del Giudice, V. Giannelli, G. Dougan, G. Douce, R. Rappuoli, and M. Pizza.** 1998. Mucosal adjuvanticity and immunogenicity of LTR72, a novel mutant of *Escherichia coli* heat-labile enterotoxin with partial knockout of ADP-ribosyltransferase activity. J. Exp. Med. **187:**1123–1132.
19. **Grossi, S. G., and R. J. Genco.** 1998. Periodontal disease and diabetes mellitus: a two-way relationship. Ann. Periodontol. **3:**51–61.
20. **Hagiwara, Y., T. Iwasaki, H. Asanuma, Y. Sato, T. Sata, C. Aizawa, T. Kurata, and S. Tamura.** 2001. Effects of intranasal administration of cholera toxin (or *Escherichia coli* heat-labile enterotoxin) B subunits supplemented with a trace amount of the holotoxin on the brain. Vaccine **19:**1652–1660.
21. **Hamada, N., K. Watanabe, T. Tahara, K. Nakazawa, I. Ishida, Y. Shibata, T. Kobayashi, H. Yoshie, Y. Abiko, and T. Umemoto.** 2007. The r40-kDa outer membrane protein human monoclonal antibody protects against *Porphyromonas gingivalis*-induced bone loss in rats. J. Periodontol. **78:**933–939.
22. **Hamajima, S., M. Maruyama, T. Hijiya, H. Hatta, and Y. Abiko.** 2007. Egg yolk-derived immunoglobulin (IgY) against *Porphyromonas gingivalis* 40-kDa outer membrane protein inhibits coaggregation activity. Arch. Oral Biol. **52:**697–704.
23. **Hiratsuka, K., Y. Abiko, M. Hayakawa, T. Ito, H. Sasahara, and H. Takiguchi.** 1992. Role of *Porphyromonas gingivalis* 40-kDa outer membrane protein in the aggregation of *P. gingivalis* vesicles and *Actinomyces viscosus*. Arch. Oral Biol. **37:**717–724.
24. **Holt, S. C., L. Kesavalu, S. Walker, and C. A. Genco.** 1999. Virulence factors of *Porphyromonas gingivalis*. Periodontol. 2000 **20:**168–238.
25. **Katoh, M., S. Saito, H. Takiguchi, and Y. Abiko.** 2000. Bactericidal activity of a monoclonal antibody against a recombinant 40-kDa outer membrane protein of *Porphyromonas gingivalis*. J. Periodontol. **71:**368–375.
26. **Kawamoto, Y., M. Hayakawa, and Y. Abiko.** 1991. Purification and immunochemical characterization of a recombinant outer membrane protein from *Bacteroides gingivalis*. Int. J. Biochem. **23:**1053–1061.
27. **Kelso, J. M., R. T. Jones, and J. W. Yunginger.** 1993. Anaphylaxis to measles, mumps, and rubella vaccine mediated by IgE to gelatin. J. Allergy Clin. Immunol. **91:**867–872.
28. **Kinane, D. F.** 1998. Periodontal diseases' contributions to cardiovascular disease: an overview of potential mechanisms. Ann. Periodontol. **3:**142–150.
29. **Klausen, B., R. T. Evans, and C. Sfintescu.** 1989. Two complementary methods of assessing periodontal bone level in rats. Scand. J. Dent. Res. **97:**494–499.
30. **Koizumi, Y., T. Kurita-Ochiai, and M. Yamamoto.** 2008. Transcutaneous immunization with an outer membrane protein of *Porphyromonas gingivalis* without adjuvant elicits marked antibody responses. Oral Microbiol. Immunol. **23:**131–138.
31. **Kolenbrander, P. E., and R. N. Andersen.** 1984. Cell to cell interactions of *Capnocytophaga* and *Bacteroides* species with other oral bacteria and their potential role in development of plaque. J. Periodontal Res. **19:**564–569.
32. **Kweon, M. N., M. Yamamoto, M. Kajiki, I. Takahashi, and H. Kiyono.** 2000. Systemically derived large intestinal $CD4^+$ Th2 cells play a central role in STAT6-mediated allergic diarrhea. J. Clin. Investig. **106:**199–206.
33. **Kweon, M. N., M. Yamamoto, F. Watanabe, S. Tamura, F. W. Van Ginkel, A. Miyauchi, H. Takagi, Y. Takeda, T. Hamabata, K. Fujihashi, J. R. McGhee, and H. Kiyono.** 2002. A nontoxic chimeric enterotoxin adjuvant induces protective immunity in both mucosal and systemic compartments with reduced IgE antibodies. J. Infect. Dis. **186:**1261–1269.
34. **Lalla, E., I. B. Lamster, M. A. Hofmann, L. Bucciarelli, A. P. Jerud, S. Tucker, Y. Lu, P. N. Papapanou, and A. M. Schmidt.** 2003. Oral infection with a periodontal pathogen accelerates early atherosclerosis in apolipoprotein E-null mice. Arterioscler. Thromb. Vasc. Biol. **23:**1405–1411.
35. **Lycke, N., T. Tsuji, and J. Holmgren.** 1992. The adjuvant effect of *Vibrio cholerae* and *Escherichia coli* heat-labile enterotoxins is linked to their ADP-ribosyltransferase activity. Eur. J. Immunol. **22:**2277–2281.
36. **Maeba, S., S. Otake, J. Namikoshi, Y. Shibata, M. Hayakawa, Y. Abiko, and M. Yamamoto.** 2005. Transcutaneous immunization with a 40-kDa outer membrane protein of *Porphyromonas gingivalis* induces specific antibodies which inhibit coaggregation by *P. gingivalis*. Vaccine **23:**2513–2521.
37. **Maiden, M. F., R. J. Carman, M. A. Curtis, I. R. Gillett, G. S. Griffiths, J. A. Sterne, J. M. Wilton, and N. W. Johnson.** 1990. Detection of high-risk groups and individuals for periodontal diseases: laboratory markers based on the microbiological analysis of subgingival plaque. J. Clin. Periodontol. **17:**1–13.
38. **Marinaro, M., H. F. Staats, T. Hiroi, R. J. Jackson, M. Coste, P. N. Boyaka, N. Okahashi, M. Yamamoto, H. Kiyono, H. Bluethmann, et al.** 1995. Mucosal adjuvant effect of cholera toxin in mice results from induction of T helper 2 (Th2) cells and IL-4. J. Immunol. **155:**4621–4629.
39. **Mealey, B. L.** 1999. Influence of periodontal infections on systemic health. Periodontol. 2000 **21:**197–209.
40. **Messer, H. H.** 1980. Alveolar bone loss in a strain of mice. J. Periodontal Res. **15:**193–205.
41. **Meyer, D. H., and P. M. Fives-Taylor.** 1998. Oral pathogens: from dental plaque to cardiac disease. Curr. Opin. Microbiol. **1:**88–95.
42. **Miyauchi, A., M. Ozawa, M. Mizukami, K. Yashiro, S. Ebisu, T. Tojo, T. Fujii, and H. Takagi.** 1999. Structural conversion from non-native to native form of recombinant human epidermal growth factor by *Brevibacillus choshinensis*. Biosci. Biotechnol. Biochem. **63:**1965–1969.
43. **Namikoshi, J., S. Otake, S. Maeba, M. Hayakawa, Y. Abiko, and M. Yamamoto.** 2003. Specific antibodies induced by nasally administered 40-kDa outer membrane protein of *Porphyromonas gingivalis* inhibit coaggregation activity of *P. gingivalis*. Vaccine **22:**250–256.
44. **Pizza, M., M. R. Fontana, M. M. Giuliani, M. Domenighini, C. Magagnoli, V. Giannelli, D. Nucci, W. Hol, R. Manetti, and R. Rappuoli.** 1994. A genetically detoxified derivative of heat-labile *Escherichia coli* enterotoxin induces neutralizing antibodies against the A subunit. J. Exp. Med. **180:**2147–2153.
45. **Reddy, M. S.** 2002. Oral osteoporosis: is there an association between periodontitis and osteoporosis? Compend. Contin. Educ. Dent. **23:**21–28.
46. **Saito, S., M. Hayakawa, K. Hiratsuka, H. Takiguchi, and Y. Abiko.** 1996. Complement-mediated killing of *Porphyromonas gingivalis* 381 by the immunoglobulin G induced by recombinant 40-kDa outer membrane protein. Biochem. Mol. Med. **58:**184–191.
47. **Saito, S., K. Hiratsuka, M. Hayakawa, H. Takiguchi, and Y. Abiko.** 1997. Inhibition of a *Porphyromonas gingivalis* colonizing factor between *Actinomyces viscosus* ATCC 19246 by monoclonal antibodies against recombinant 40-kDa outer-membrane protein. Gen. Pharmacol. **28:**675–680.